Brain, Behavior, and Immunity 137 (2026) 106820

Contents lists available at ScienceDirect

Brain Behavior and Immunity

journal homepage: www.elsevier.com/locate/ybrbi

Full-length Article

Early IL17A blockade following maternal immune activation prevents behavioral abnormalities, hippocampal synaptic changes and neuroinflammation in male and female offspring

Maria Stefania Spagnuolo [a,1], Giorgia Macchioni [b,c,1], Natasha Petecca [d], Giulia Petruccioli [b], Mattia De Magistris [b], Francesca De Palma [d], Marina Prisco [d], Chiara Cipriani [e], Martina Siracusano [f], Gemma Calamandrei [b], Laura Ricceri [b], Luisa Cigliano [d,g,2,*], Anna Maria Tartaglione [b,2,**]

[a] Institute for the Animal Production System in the Mediterranean Environment, National Research Council, Piazzale Enrico Fermi 1, 80055 Portici, Italy
[b] Centre for Behavioral Sciences and Mental Health, Istituto Superiore di Sanità (ISS), Viale Regina Elena, 299, 00161 Rome, Italy
[c] Department of Physiology and Pharmacology "V. Erspamer", Sapienza University of Rome, Piazzale Aldo Moro, 5, 00185 Rome, Italy
[d] Department of Biology, University of Naples Federico II, Complesso Universitario Monte S. Angelo, Edificio 7, Via Cintia, 80126 Naples, Italy
[e] Department of Experimental Medicine, University of Rome Tor Vergata, Via Montpellier, 1, 00133 Rome, Italy
[f] Department of Biomedicine and Prevention, University of Rome Tor Vergata, Via Montpellier, 1, 00133 Rome, Italy
[g] Task Force on Microbiome Studies, University of Naples Federico II, 80126 Naples, Italy

ARTICLE INFO

Keywords:
Maternal immune activation
Inflammation
Autism Spectrum Disorder
Synaptic protein
Brain derived neurotrophic factor
Behavior
Mouse model

ABSTRACT

Autism Spectrum Disorder (ASD) is marked by impairments in social communication and interaction, alongside repetitive behavior, with increasing evidence implicating immune dysregulation in its pathogenesis. Preclinical studies indicate that infections during pregnancy and resultant maternal immune activation (MIA) induces ASD-like neurobehavioral abnormalities in offspring, involving interleukin-17A (IL17A) released by T helper 17 cells. Here, we evaluated the potential efficacy of early administration of IL17A antibody shortly after MIA induction to mitigate ASD-like phenotypes focusing on both male and female mouse offspring.

MIA was induced by administering polyinosinic:polycytidylic acid [Poly(I:C)] to pregnant mice on gestational day 12.5. Twenty-four hours later, mice were injected with IL17A antibody (anti-IL17A). Offspring were divided into three developmental cohorts (neonatal, early adolescence, and late adolescence), each tested with a tailored behavioral battery relevant to ASD. Additionally, to get further insight into MIA-induced molecular changes and the potential efficacy of anti-IL17A treatment in preventing these effects, hippocampal synaptic and neuro-inflammatory markers were analyzed at postnatal day 28.

Prenatal administration of anti-IL17A significantly attenuated repetitive behavior selectively observed in MIA male offspring and mitigated social deficits emerging in late adolescence in both sexes. Importantly, anti-IL17A administration prevented in both sexes early MIA-induced alterations in key players of synaptic plasticity (i.e. brain derived neurotrophic factor, synaptic proteins, glutamate receptor NMDA) and neuroinflammation.

Early and precisely timed blockade of IL17A (24 h after MIA-induction) represents a promising prophylactic strategy to prevent ASD-like brain and behavioral abnormalities associated with MIA.

* Corresponding author at: Department of Biology, University of Naples Federico II, Complesso Universitario Monte S. Angelo, Edificio 7, Via Cintia, 80126 Naples, Italy.
** Corresponding author.
E-mail addresses: luisa.cigliano@unina.it (L. Cigliano), annamaria.tartaglione@iss.it (A.M. Tartaglione).
[1] These authors contributed equally (co-first authors).
[2] These authors contributed equally (co-last authors).

https://doi.org/10.1016/j.bbi.2026.106820
Received 15 January 2026; Received in revised form 30 April 2026; Accepted 18 May 2026
Available online 21 May 2026

1. Introduction

Autism spectrum disorder (ASD) is sex-biased, neurodevelopmental disorder characterized by social and communication impairments and repetitive behavior (Association, 2013). It is associated with alterations in brain physiology, involving molecular and cellular hallmarks (Gilbert and Man, 2017; Toscano et al., 2021). Maternal factors such as stress, exposure to chemicals and drugs, overnutrition, inflammation and infection during pregnancy may negatively impact brain development during fetal life, increasing the risk of ASD (Jiang et al., 2016; Kwon et al., 2022) as well as other psychiatric and neurological disorders. In particular, epidemiological studies have linked maternal infection to ASD as well as to neuropsychiatric conditions, such as intellectual disability, schizophrenia, bipolar disorder, and major depressive disorder (Brown and Meyer, 2018; Jiang et al., 2016; Kwon et al., 2022; Meyer, 2019; Meyer et al., 2011; Meyer et al., 2009a). Animal models of maternal immune activation (MIA) have been used to investigate the causal link between maternal infection and abnormal brain development in the offspring, in terms of behavioral, neurochemical, neuroanatomic, and neurophysiologic disruptions (Brown and Meyer, 2018; Malkova et al., 2012; Meyer, 2014; Meyer and Feldon, 2010, 2012; Meyer et al., 2009a; Sal-Sarria et al., 2024). Rodent models of MIA, induced by injection of the synthetic double stranded RNA polyinosinic-polycytidylic acid [Poly(I:C)], widely used to mimic viral infection, recapitulate the association between maternal infection and offspring brain and behavioral alterations resembling core features of ASD. In these models, MIA elevates proinflammatory cytokines, which, depending on cytokine specificity, timing of MIA, gestational stage, and concomitant placental abnormalities, can cross the placenta and directly affect the embryonic brain (Meyer et al., 2009b; Meyer et al., 2007). This triggers neuroinflammation that can persist into later developmental stages, contributing to aberrant behavioral phenotypes in offspring (Arrode-Bruses and Bruses, 2012; Garcia-Valtanen et al., 2020; Haddad et al., 2020; Malkova et al., 2012; Tartaglione et al., 2022). T helper 17 cells and their effector interleukin-17A (IL17A) have been identified as critical mediators in the development of MIA-induced behavioral abnormalities in offspring (Choi et al., 2016). Elevated IL17A levels have been reported in both maternal blood and the postnatal brain of MIA mouse models (Choi et al., 2016; Garay et al., 2013). Importantly, higher blood IL17A levels correlated with phenotypic severity in a subset of ASD subjects (Wong and Hoeffer, 2018). Despite evidence supporting IL17A as a potential therapeutic target (Choi et al., 2016), critical issues, such as the optimal time window for intervention and the appropriate period to observe its effects on molecular and behavioral alterations in Poly(I:C)-exposed offspring, remain less explored. Furthermore, given the pronounced sex bias in ASD prevalence, most studies have focused predominantly on males, leaving a gap in the understanding of the mechanisms underlying sex-specific responses to early-life inflammatory insults leading to this disease. Also, no data are available on both sexes in response to anti-IL17A in offspring as a preventive approach. Therefore, we evaluated the efficacy of an IL17A-blocking antibody administered 24 h after maternal Poly(I:C) injection in preventing ASD-like behavioral abnormalities in both male and female offspring across developmental stages. This study also enables the exploration of whether MIA-induced phenotypes are mediated by shared or divergent pathways across sexes. Since early adolescence is a critical period of synaptic pruning and stabilization in rodents, synaptic and neuroinflammatory markers were examined in hippocampus, a vulnerable area in MIA models (Ito et al., 2010; Oh-Nishi et al., 2010; Sal-Sarria et al., 2024) at postnatal day 28 (PND 28). This time point was indeed selected to assess early MIA molecular alterations as well as the potential preventive activity of anti-IL17A.

2. Materials and methods

2.1. Animals and treatments

Experimental procedures were approved by the Italian Ministry of Health (authorization no. 279/2023-PR) in full compliance with Directive 2010/63/EU. Six-week-old female and male CD1 mice (ENVIGO San Pietro al Natisone, Italy) were housed under standard conditions (temperature 21 ± 1 °C and relative humidity 60 ± 10%) with a 12:12 reversed light cycle (lights on at 7:00P.M.), with a density of 2 animals per cage.

After 2 weeks of habituation, the animals were bred (two females with one male), and females were checked twice daily for the presence of vaginal plug, designated as gestational day 0.5 (GD 0.5). At GD 12.5 pregnant mice were randomly divided in two groups: one group received a single intraperitoneal (i.p.) injection of 20 mg/kg Poly(I:C) (0.01 ml/g, InvivoGen Low Molecular Weight Poly I:C Lot#5936–45–0), while the other group received an equivalent volume of saline (0.9% NaCl). This dose was selected based on established MIA protocols, including our prior studies (Cipriani et al., 2022; Tartaglione et al., 2022), to elicit a neuroinflammatory response and reproducible ASD-like behavioral phenotypes in the offspring. On GD 13.5, each group was further subdivided to receive a second i.p. injection of either a monoclonal IL17A blocking antibody (clone 50104; R&D) or an isotype control antibody (clone 54447; R&D), both at a dose of 500 μg per mouse. The day of birth was designated as PND 0. Dam body weight after treatments, litter size, sex ratio, and mean pup body weight at PND 1 were recorded to assess potential effects of Poly(I:C) or IL17A antibody on gestational and reproductive performance. To minimize variability related to litter size, litters were culled to ten pups, maintaining, whenever possible, an equal sex ratio of five males and five females. Offspring were weaned at PND 21. For each analysis, only one pup per sex from each litter was used to limit the litter effect. A schematic representation of experimental design is presented in Fig. 1.

2.2. Behavioral testing

All behavioral tests, except for the open-field test, which was automatically tracked using ANY-maze software (Stoelting Europe, Dublin, Ireland), were video recorded and subsequently analyzed using The Observer XT-17 software (Noldus, Wageningen, The Netherlands).

2.2.1. Cohort 1: Neonatal assessment

Cohort 1 (n = 86) comprised male (M) and female (F) animals from four experimental groups: C (n = 10 M, 10 F); C-Ab (n = 10 M, 10 F); MIA (n = 10 M, 10 F); and MIA-Ab (n = 13 M, 13 F).

Both male and female pups were assessed for spontaneous motor activity and ultrasonic vocalizations (USVs) on PND 4, 7, and 10, as previously described (Tartaglione et al., 2019).

On each testing day, a single pup was placed in an empty glass container (diameter: 5 cm; height: 10 cm) positioned inside a sound-attenuating Styrofoam box for a 3-minute observation period. An ultrasound microphone (Avisoft UltrasoundGate CM16 condenser microphone capsule, Avisoft Bioacoustics, Berlin, Germany), sensitive to frequencies between 10 and 180 kHz, was inserted from above through an opening in the box cover, approximately 20 cm above the pup, to record USVs. Motor patterns analyzed included pivoting (laterally directed movements involving the forelimbs alone), locomotion (activity involving both forelimbs and hindlimbs), and curling (side-to-side rolling movements on the back). USVs emitted were quantified using DeepSqueak (Coffey et al., 2019).

On PND 12, pups underwent the homing test to assess their ability to seek and recognize familiar olfactory cues. After 30-min isolation period, each pup was placed in a polycarbonate cage (29.5 × 13 × 11.5 cm) with the floor three-quarters covered with clean bedding, leaving the remaining quarter filled with bedding collected from the pup's home

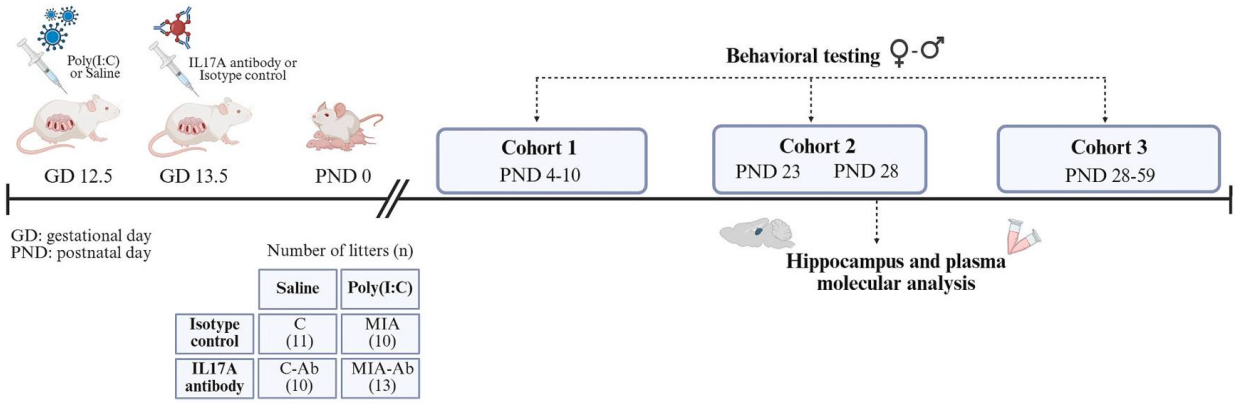

Fig. 1. Timeline of the experimental design. Pregnant dams received Poly(I:C) or saline on gestational day (GD) 12.5, followed by IL17A blocking antibody or isotype control on GD 13.5, yielding four groups: (C) saline/Isotype control; (MIA) Poly(I:C)/isotype control; (C-Ab) saline/anti-IL17A; (MIA-Ab) Poly(I:C)/anti-IL17A. Offspring of both sexes were assigned to three cohorts, each undergoing behavioral testing at distinct developmental stages: neonatal (Cohort 1; postnatal day, PND 4–10), early adolescence (Cohort 2; PND 23, followed by molecular analyses at PND 28), and early to late adolescence (Cohort 3; PND 28–59).

cage (the "nest area") to provide a familiar scent cue. The pup was placed opposite the nest area, and latency to reach it was recorded, with a 3-min cutoff.

2.2.2. Cohort 2: Early adolescence assessment

Cohort 2 (n = 63) comprised animals of both sexes from four experimental groups: C (n = 8 M, 8 F); C-Ab (n = 8 M, 8 F); MIA (n = 8 M, 7 F); and MIA-Ab (n = 8 M, 8 F).

At PND 23, repetitive behavior was assessed using the grooming test. Each mouse was placed into a clean cage (29.5 × 13 × 11.5 cm) covered with a thin layer of clean sawdust to minimize excessive digging. After 10 min of habituation, the number of self-grooming episodes (i.e., bouts > 7 s) and time spent grooming were recorded during the following 10 min. In addition, the number of transitions between grooming body regions (i.e., paws/nose, head, body, anogenital/tail) relative to the total number of bouts was analyzed.

After a 20-minute grooming test session, a social stimulus, a conspecific of the same age and sex who had been previously isolated in a separate cage for 15 min, was introduced into the test cage for an additional 5 min. The following parameters were analyzed: duration of sniffing the social stimulus (categorized as head, body, and anogenital sniffing), self-grooming, and the total USVs emitted.

2.2.3. Cohort 3: Early to late adolescence assessment

Cohort 3 (n = 86) comprised animals of both sexes from four experimental groups: C (n = 10 M, 10 F); C-Ab (n = 9 M, 10 F); MIA (n = 11 M, 11 F); and MIA-Ab (n = 13 M, 12 F).

At PND 28 and 35, animals underwent social interaction and grooming tests, respectively. Protocols and equipment were identical to those for Cohort 2, except that the social interaction test used a treatment-matched conspecific rather than a control mouse.

To further assess repetitive behavior, mice were subjected to the marble burying test at PND 48 (Coppola et al., 2026). The test was conducted in a clean cage (36 × 20.5 × 18.5 cm) filled with sawdust bedding to a depth of 5 cm, with twenty identical blue glass marbles (1.2 cm diameter) arranged in a 4 × 5 matrix on the bedding surface. Each mouse was placed in the center of the cage and allowed to explore freely for 30 min. The number of marbles buried during the test was recorded. A marble was considered buried when more than two-thirds of its surface area was covered by sawdust.

To evaluate locomotor activity and anxiety-like behavior, mice were tested in the open-field test at PND 52 (Tartaglione et al., 2022). The apparatus consisted of a black Plexiglas box (40 × 40 × 40 cm), with the arena virtually divided into central and peripheral zones. Each animal was placed in a corner of the box and allowed to explore for 10 min. Distance traveled and time spent in each zone were automatically recorded. To evaluate social approach and preference, mice underwent the three-chamber social test at PND 59. The apparatus consisted of a Plexiglas box (60 × 40 × 40 cm) divided into three interconnected chambers. After an 8-minute habituation to the empty apparatus, the subject was confined to the center chamber. An object enclosed in an inverted wire cup was placed in one side chamber, while an unfamiliar, age- and sex-matched mouse was enclosed under an identical wire cup in the opposite chamber. The subject was then allowed to explore all chambers for 3 min. The locations of the object and social stimulus were counterbalanced across subjects. Time spent in each chamber and time sniffing each cup were recorded. Sociability preference index (%) was calculated using the following formula: (S/(S + O)) × 100 where S = time sniffing social stimulus/time spent in social chamber and O = time sniffing object/time spent in object chamber.

2.3. Sample collection

At PND 28, mice from Cohort 2 were euthanized by decapitation, and blood and hippocampal tissues were collected. This time point was selected to capture an early adolescent phase at which hippocampal synaptic refinement is still prominent (Filipello et al., 2018; Milbocker et al., 2021; Paolicelli et al., 2011; Semple et al., 2013), during which the MIA effects on synaptic development are particularly evident (Dutra et al., 2023; Mirabella et al., 2021; Oh-Nishi et al., 2010).

Blood samples were collected in EDTA-coated tubes and centrifuged (1100 × g, 15 min, 4 °C). The resulting plasma and hippocampal samples were stored at −80 °C until further analyses or immediately fixed in paraformaldehyde (4% in PBS) for immunofluorescence investigation.

2.4. Preparation of hippocampus protein extracts

Aliquots (15 mg) of frozen hippocampus were homogenized in seven volumes of RIPA buffer (150 mM NaCl, 50 mM Tris- HCl pH 8.0, 0.5% sodium deoxycholate, 0.5% NP-40, 0.1% SDS) containing 1% Protease Inhibitor Cocktail and 1% Phosphatase Inhibitor Cocktail (Euroclone, Milan, Italy) as previously reported (Spagnuolo et al., 2014).

2.5. ELISA

Plasma and hippocampus concentrations of tumor necrosis factor-alpha (TNF-alpha) and interleukin-6 (IL-6) were assessed using a sandwich enzyme-linked immunosorbent assay (R&D Systems, Minneapolis, MN, USA) specific for mouse, in agreement with the manufacturer instructions, in samples dilutes 1:15 (plasma) or 1:80 (hippocampus).

IL17A was titrated, in samples dilutes 1:20 (plasma) or 1:60 (hippocampus), using a sandwich enzyme-linked immunosorbent assay (Biolegend, San Diego, CA, USA) specific for mouse, in agreement with the manufacturer instructions.

2.6. Western blotting

Denaturing and reducing electrophoresis of hippocampal extracts (Spagnuolo et al., 2018) was carried out on 12.5% polyacrylamide gels to titrate post-synaptic density protein 95 (PSD-95), synaptosome-associated protein 25 (SNAP-25), synaptotagmin, brain derived neurotrophic factor (BDNF), fractalkine receptor (CX3CR1), apolipoprotein E (ApoE) or on 10% to assay toll-like receptor-4 (TLR4), myeloid differentiation factor 88 (MyD88), nuclear factor kappa-light-chain-enhancer of activated B cells (NFkB), glial fibrillary acidic protein (GFAP), N-methyl-D-aspartic acid receptor (NMDA-R), liver X receptor (LXR), ABC Transporter A1 (ABCA-1). Proteins blotting onto nitrocellulose membrane (Amersham Protran; Euroclone, Milan, Italy), washing and blocking steps were carried out according to previously published procedures (Spagnuolo et al., 2018). After blocking, the membranes were incubated with primary antibodies (overnight, at 4 °C), washed and then treated (1 h, at 37 °C) with the appropriate peroxidase-conjugated secondary antibodies (Supplementary Table 1). The amount of phosphorylated NFkB was expressed as relative to total NFkB, so, after revelation of the immunocomplexes, the membranes were submerged in stripping buffer (1% SDS, 25 mM Glycine, pH 2; 30 min, 37 °C) (Spagnuolo et al., 2018), extensively washed, and then incubated with the specific antibody for the total form of NFkB (Supplementary Table 1). For loading control, after detection of each antigen, the membranes were stripped and incubated (overnight, 4 °C) with mouse anti-β-actin IgG followed by goat anti mouse (GAM)-HRP IgG (see Supplementary Table 1). Signal detection was carried out using the Excellent Chemiluminescent Kit from Elabscience (cat# E-IR-R301). Densitometric analysis of chemidoc or digital images of X-ray films exposed to immunostained membranes was performed with Un-Scan-It gel software (Silk Scientific, UT, USA). Most gels were run with sex matched samples. When male and female samples were run on separated gels, at least one sample from the opposite sex was loaded, as reference point, to allow for normalization across gels and enable statistical comparison between male and female groups.

2.7. Immunofluorescence analysis

Hippocampus was isolated, fixed in paraformaldehyde (4% in PBS) dehydrated in a series of increasing concentrations of alcohol, and embedded in paraffin. The immunodetection was carried out on sections (5 μm thick) of dentate gyrus with a rabbit anti-Iba 1 antibody (Cell Signaling Technology) diluted 1:200 in blocking solution (PBS-Tween 0.1% − BSA 3%; overnight at 4 °C) and an anti-rabbit secondary antibody conjugated to Dylight 594 (ImmunoReagents, Raleigh, USA; cat # GtxRb-003-D594NHSX; diluted 1:200 in blocking solution; 1 h at room temperature). Sections 5 μm thick were mounted on poly-lysine-coated slides, deparaffinized, rehydrated, and brought to water. The slides were mounted with Mowiol and observed under a Zeiss Axioskop fluorescence microscope; the images were acquired with Zeiss ZEN 3.8 software. For each sample, five photographic fields acquired at 20x magnification were analyzed. The analysis of relative fluorescence intensity was carried out with Image J software: integrated density values were compared and plotted on graphs, expressed in arbitrary units.

2.8. Statistical analysis

Data were analyzed using GraphPad Prism 9.3.1 (GraphPad Software, San Diego, CA, USA). Depending on the distribution of the response variable, data were analyzed using either a three-way ANOVA with condition (saline vs Poly(I:C)), treatment (isotype vs anti-IL17A), and sex (male vs female) as fixed independent variables (including repeated measures for PND during neonatal testing) or a Kruskal–Wallis test. Post hoc analyses for multiple comparisons were performed using Tukey's or Dunn's tests, respectively. One-sample *t*-test versus chance level, followed by Bonferroni correction, were also applied. Spearman correlations were conducted to evaluate the relationships between molecular markers and behavioral parameters, either across all animals irrespective of condition and treatment, stratified by sex, or within each condition and treatment group for each sex.

3. Results

3.1. MIA affects early motor patterns in male offspring with modulation by anti-IL17A treatment

Gestational Poly(I:C) administration, anti-IL17A treatment, or their interaction did not significantly influence gestation length, litter size, sex ratio, or pup body weight on PND 1 (Supplementary Fig. 1). Analysis of spontaneous motor activity from PND 4 to PND 10 (Cohort 1) revealed a selective effect of MIA on the duration of curling, defined as vigorous side-to-side rolling movements performed by the pup while lying on its back, and pivoting, an immature motor pattern progressively replaced by quadrupedal locomotion during development.

Curling analysis was focused on PND 4, as this behavior was very sporadic or absent at PND 7 and PND 10, coinciding with the progressive development of motor coordination. MIA significantly increased the curling duration in offspring of both sexes [main effect of condition, $F(1,74) = 4.784$, $p = 0.0319$], regardless of treatment. This motor pattern was not significantly modulated by anti-IL17A [main effect of treatment, $F(1,38) = 3.441$, $p = 0.0714$, Fig. 2A]. Moreover, pivoting duration was significantly increased in male MIA offspring compared to controls across the PNDs [MIA males vs C males: $p < 0.05$ following Tukey's test, condition × treatment × sex interaction, $F(1,77) = 4.105$, $p = 0.0462$, Fig. 2B], indicating a hyperactivity-like phenotype that was not prevented by anti-IL17A treatment.

By contrast, a modulatory effect of the anti-IL17A was observed on quadrupedal locomotion, with treatment reducing its duration in females but not in males [C-Ab and MIA-Ab females vs. C and MIA females: $p < 0.01$ following Tukey's test, treatment × sex interaction, $F(1,78) = 5.578$, $p = 0.0207$, Fig. 2C]. Additionally, the number of USVs emitted during brief isolation from the dam and littermates, which is an early indicator of socio-communicative competence, was significantly reduced by anti-IL17A in animals of both sexes [main effect of treatment, $F(1,78) = 10.248$, $p = 0.0020$, Fig. 2D].

Neither MIA nor anti-IL17A affected the latency to reach the nest area in the Homing test at PND 12, indicating comparable abilities across experimental groups in seeking and recognizing an early salient social cue [$H = 3.528$, $p = 0.8323$, Supplementary Fig. 2].

3.2. Anti-IL17A treatment prevents ASD-like behavioral changes in MIA offspring

At the beginning of the post-weaning stage (PND 23, Cohort 2), MIA offspring did not exhibit significant ASD-like behavioral abnormalities, except for the increase in self-grooming observed exclusively in males, but during social interaction [$p < 0.05$ compared to C following Dunn's test, $H = 20.56$, $p = 0.0045$]. This phenotype, indicative of heightened repetitive behaviors in response to social stimuli, was not reversed by anti-IL17A (Supplementary Fig. 3).

Given the significant main effect of sex and the absence of interactions with condition and/or treatment on self-grooming duration [$F(1,77) = 4.836$, $p = 0.0309$] in the grooming test (PND 35, Cohort 3), data were analyzed separately by sex. Specifically, MIA males, but not females, displayed elevated grooming levels compared to control males [main effect of condition, $F(1,38) = 4.297$, $p = 0.0450$, Fig. 3A], regardless of the treatment received, in a non-social environment.

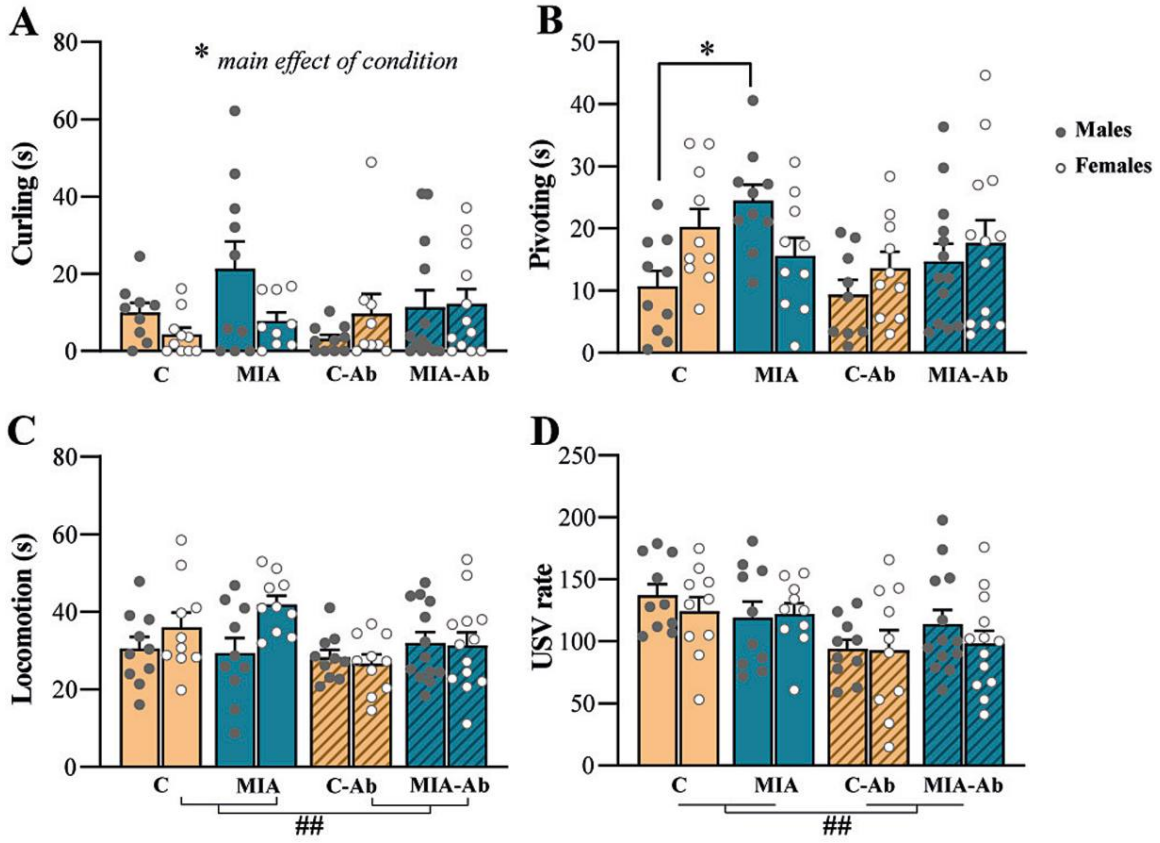

Fig. 2. Cohort 1_Spontaneous motor activity and ultrasonic vocalizations (USVs) at postnatal days (PND) 4, 7, and 10. Curling duration at PND 4 (A). Pivoting duration across PNDs (B). Locomotion duration across PNDs (C). Number of USVs across PNDs (D). Data are presented as mean ± SEM, with individual data points shown as dots; n = 10–13 per group/sex; C: saline/isotype control, MIA: Poly(I:C)/isotype control, C-Ab: saline/anti-IL17A, MIA-Ab: Poly(I:C)/anti-IL17A. *p < 0.05, MIA and MIA-Ab vs. C and C-Ab (A); *p < 0.05 MIA males vs C males (B); $^{\#\#}$p < 0.01, C-Ab and MIA-Ab females vs. C and MIA females (C); $^{\#\#}$p < 0.01, C-Ab and MIA-Ab vs. C and MIA (D) (Three-way ANOVA followed by Tukey's post-hoc test).

Additionally, a main effect of treatment was observed, as anti-IL17A administration was associated with overall lower grooming levels [F (1,38) = 4.454, p = 0.0415, Fig. 3A]. Consistently, only MIA males showed a higher number of grooming transitions compared to control males, regardless of treatment [p < 0.05 following Tukey's test, condition × sex interaction, F(1,76) = 6.656, p = 0.0118]. Notably, anti-IL17A treatment was associated with fewer transitions in males but not in females [C-Ab and MIA-Ab males vs. C and MIA males: p < 0.05 following Tukey's test, treatment × sex interaction, F(1,76) = 5.614, p = 0.0204, Fig. 3B]. Interestingly, the impact of MIA condition and anti-IL17A on self-grooming in males was not reflected in repetitive behaviors assessed by the marble burying test, where no significant effect on the number of marbles buried was observed (Supplementary Fig. 4).

Similarly to Cohort 2, animals within this cohort, paired with social partners matched by treatment group to detect even subtle variations in reciprocal social interaction, did not exhibit social and communicative deficits (Supplementary Fig. 4).

In late adolescence, social preference was assessed in the three-chamber social test. A main effect of treatment on the social preference index was observed [F(1, 68) = 6.160, p = 0.0155, Fig. 3C], with anti-IL17A-treated mice of both sexes showing higher preference for the social stimulus than those receiving isotype control. As expected, control male mice exhibited a preference for the social stimulus over the object [C: t(8) = 4.422, p = 0.0022, p adj = 0.0176 vs. 50% chance level; C-Ab: t(8) = 3.301, p = 0.0108, p adj = 0.0864]. MIA condition in males induced a marked deficit in social preference [MIA: t(8) = 1.153, p = 0.2822, p adj = 2.2576], which was prevented by anti-IL17A [MIA-Ab: t (11) = 4.027, p = 0.0020, p adj = 0.0161]. A similar pattern was observed in females [C: t(7) = 6.721, p = 0.0003, p adj = 0.0024; C-Ab: t (9) = 6.482, p = 0.0001, p adj = 0.0008; MIA: t(8) = 2.117, p = 0.0672, p adj = 0.5376; MIA-Ab: t(9) = 4.542, p = 0.0014, p adj = 0.0112 vs. 50% chance level, Fig. 3C].

Total distance traveled and time spent in the open-field centre were unaffected by MIA or anti-IL17A (Fig. 3D–E), indicating that the three-chamber effects were specific to the social domain rather than to altered locomotion or anxiety-like behavior.

3.3. *Anti-IL17A treatment prevents MIA-induced decrease of synaptic function markers*

Previous studies revealed hippocampal synaptic dysregulation in MIA offspring (Page et al., 2021; Yotova et al., 2024). Early MIA-induced synaptic protein alterations in male and female offspring and the putative efficacy of anti-IL17A were therefore investigated.

Within each sex, the amount of the mature form of BDNF, a key neurotrophin involved in a wide range of neurophysiological processes including synaptic protein expression (Barde, 2025), was reduced in hippocampus of MIA compared to C mice [p < 0.01 following Tukey's test, Fig. 4A]. Importantly, anti-IL17A prevented BDNF level changes in MIA male and female offspring [p < 0.01following Tukey's test; condition × treatment interaction, F (1,52) = 19.31, p < 0.0001, Fig. 4A] but had no effect in controls.

We also evaluated the amounts of two pre-synaptic proteins, namely SNAP-25 and synaptotagmin I, and the post-synaptic protein PSD-95, which plays a relevant role in synaptic plasticity (Won et al., 2017). These proteins were lower in MIA than in C mice [p < 0.01 following Tukey's test, Fig. 4B–D], and anti-IL17A was able to prevent MIA-induced reduction, as higher levels were found in MIA-Ab compared

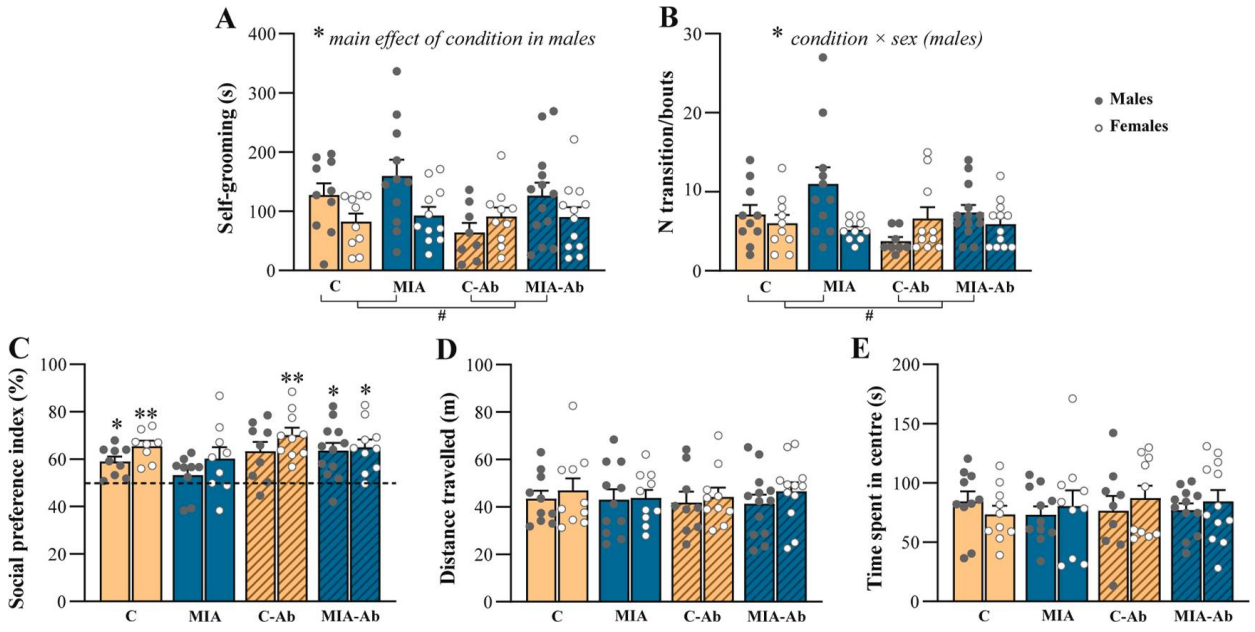

Fig. 3. Cohort 3_Behavioral assessment from postnatal day (PND) 28 to 59. Self-grooming duration (A) and number of transitions/bouts in the grooming test (B); social preference index in the three-chamber social test (C); distance travelled (D) and time spent in the centre area (E) in the open-field test. Data are presented as mean + SEM, with individual data points shown as dots; n = 9–13 per group/sex; C: saline/isotype control, MIA: Poly(I:C)/isotype control, C-Ab: saline/anti-IL17A, MIA-Ab: Poly(I:C)/anti-IL17A. *p < 0.05, C-Ab and MIA-Ab males vs. C and MIA males; #p < 0.05, C-Ab and MIA-Ab males vs. C and MIA males (A, Two-way ANOVA); *p < 0.05, MIA and MIA-Ab males vs. C and C-Ab males; #p < 0.05, C-Ab and MIA-Ab males vs. C and MIA males (B, Three-way ANOVA followed by Tukey's post-hoc test); *p < 0.05, **p < 0.01, one-sample *t*-test (vs. 50% chance level) followed by Bonferroni correction (C).

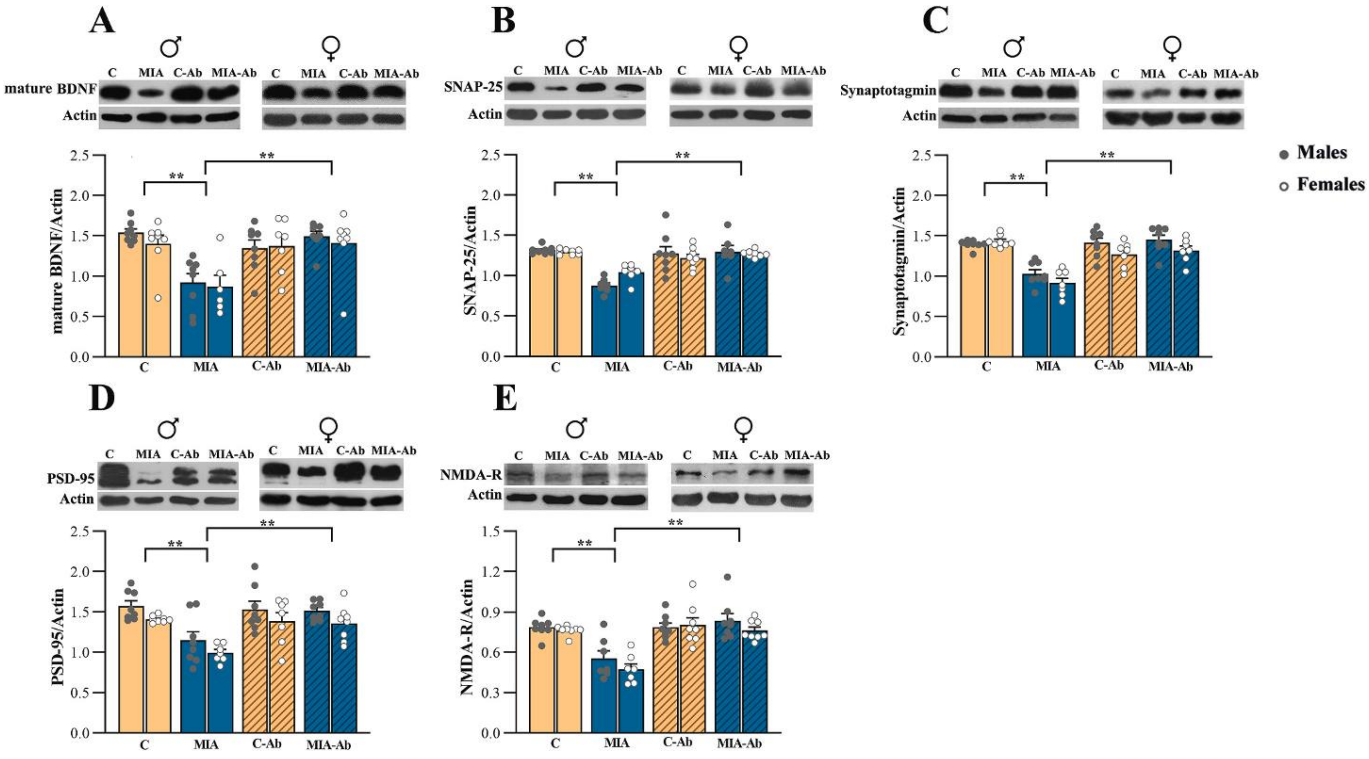

Fig. 4. Markers of hippocampus plasticity. Mature form of brain derived neurotrophic factor (BDNF; A), synaptosome-associated protein (SNAP-25; B), synaptotagmin (C), postsynaptic density protein 95 (PSD-95; D), N-methyl-D-aspartic acid receptor (NMDA-R; E). Representative blots (normalized to controls) of hippocampus from offspring prenatally treated with (C) saline/isotype control, (MIA) Poly(I:C)/isotype control, (C-Ab) saline/anti-IL17A, or (MIA-Ab) Poly(I:C)/anti-IL17A are shown. Data are presented as mean + SEM, with individual data points shown as dots; n = 7–8 per group/sex. **p < 0.01 (Three-way ANOVA followed by Tukey's post-hoc test).

to MIA mice, regardless the sex [SNAP-25: p < 0.01 following Tukey's test, condition × treatment interaction, F (1,53) = 31.55, p < 0.0001, Fig. 4B; synaptotagmin: p < 0.01 following Tukey's test, condition × treatment interaction, F (1,53) = 47.35, p < 0.0001, Fig. 4C; PSD-95: p

< 0.01 following Tukey's test, condition × treatment interaction, F (1,54) = 13.82, p = 0.0005, Fig. 4D]. No anti-IL17A effect was observed in controls (Fig. 4B-D).

Finally, the amount of the NMDA receptor subtype ε2 (GluN2B, herein indicated as NMDA-R), fundamental for dendritic morphology and synaptic function (Keith et al., 2019; Reiner and Levitz, 2018), was lower in MIA animals compared to controls [p < 0.01 following Tukey's test, Fig. 4E] with anti-IL17A preventing this reduction in MIA-Ab mice [p < 0.01 following Tukey's test, condition × treatment interaction, F (1,54) = 22.79, p < 0.0001, Fig. 4E]. The administration of anti-IL17A to controls did not affect this receptor.

3.4. MIA does not affect cholesterol homeostasis markers in offspring

Since alterations of the protein network regulating cholesterol metabolism have been described in ASD (Cartocci et al., 2018; Cartocci et al., 2019; Servadio et al., 2016; Wu et al., 2017) and associated with synaptic signaling disturbance (Cartocci et al., 2018), we investigated whether cholesterol dysregulation occurs in MIA offspring. To this aim, hippocampal levels of ApoE, a key modulator of cholesterol trafficking (Pfrieger and Ungerer, 2011; Yang et al., 2023), LXR-beta, the regulator of ApoE expression (Courtney and Landreth, 2016), and ABCA-1, involved in cholesterol efflux and ApoE lipidation (Kim et al., 2007) were measured. Cholesterol metabolism markers were not affected in hippocampus of MIA offspring compared to controls (Fig. 5A–C), suggesting that, differently from other ASD models, cholesterol metabolism markers are not affected in hippocampus of MIA offspring.

3.5. Anti-IL17A treatment prevents MIA-induced neuroinflammation

As MIA induces a prominent neuroinflammatory response in the offspring (Osman et al., 2024; Pendyala et al., 2017), the effect of prenatal anti-IL17A on multiple key mediators of this pathway was then investigated in the hippocampus. MIA offspring of both sexes showed increased NFkB phosphorylation [used as marker of its activation; p < 0.01 following Tukey's test, condition × treatment interaction, F (1,50) = 15.93, p = 0.0002, Fig. 6A], along with higher concentrations of TNF-alpha [p < 0.01 following Tukey's test, condition × treatment interaction, F (1,48) = 21.11, p < 0.0001, Fig. 6B] and IL-6 [p < 0.01 following Tukey's test, condition × treatment interaction, F (1,44) = 58.57, Fig. 6C] compared to C mice. These rises were prevented by anti-IL17A administration both in males and in females, as indicated by reduced p-NFkB/NFkB, TNF-alpha, and IL-6 levels in MIA-Ab compared to MIA mice [all p < 0.01 following Tukey's test, Fig. 6A-C].

To go further insight into the mechanistic impact of IL17A on neuroinflammation development, its protein level was titrated in hippocampus and, within each sex, a higher amount of IL17A was found in MIA compared to C mice [p < 0.01 for each sex following Tukey's test, condition × treatment × sex interaction, F (1,42) = 31.53, p < 0.0001, Fig. 6D], in line with previous reports (Choi et al., 2016; Fan et al., 2024; Gillespie et al., 2024; Wang et al., 2025). Anti-IL17A prevented this change in MIA offspring validating the efficacy of this strategy of intervention [p < 0.01 for each sex following Tukey's test, Fig. 6D] without affecting controls. Notably, IL17A was significantly higher in females than in males within each group [all p < 0.01 following Tukey's test].

Further, since hippocampal TLR4 gene upregulation has been reported in MIA-exposed offspring (Talukdar et al., 2021), we investigated whether changes of this receptor were associated to the observed inflammatory condition in our model. Interestingly, higher amounts of TLR4 and MyD88, a downstream protein of TLR4 signaling pathway, as well as GFAP, a marker of astrogliosis, were found in MIA compared to C mice [TLR4: p < 0.01 following Tukey's test, condition × treatment interaction, F (1,50) = 23.15, p < 0.0001, Fig. 7A; MyD88: p < 0.01 following Tukey's test, condition x treatment interaction, F (1,55) = 15.11, p = 0.0003, Fig. 7B; GFAP: p < 0.01 following Tukey's test, condition x treatment interaction, F (1,54) = 14.91, p = 0.0003, Fig. 7C]. Notably, MIA-induced inflammatory pathway activation was prevented by anti-IL17A [all markers: p < 0.01 following Tukey's test].

Also, the CX3CR1 receptor level was higher in MIA compared to C group [p < 0.01 following Tukey's test, condition × treatment interaction, F (1, 50) = 63.34, p < 0.0001, Fig. 7D], and prenatal IL17A blockade was able to significantly prevent its increase [p < 0.01 following Tukey's test].

Further, the expression of Iba1, a critical biomarker of microglia activation, was increased in MIA compared to C mice [p < 0.01 following Tukey's test, condition × treatment interaction, F (1,16) = 62.06, p < 0.0001, Fig. 8] and anti-IL17A was again effective in preventing this increase [p < 0.01 following Tukey's test].

Interestingly, neuroinflammation markers did not differ between C and C-Ab group (Figs. 6–8), providing evidence that anti-IL17A prevented neuroinflammation in MIA offspring without perturbing hippocampal status in control mice.

3.6. MIA is associated with IL17A levels increase in offspring plasma

Brain inflammation could derive from systemic inflammation, since increased concentration of molecular mediators of inflammation in systemic blood can drive their increase also in the brain (D'Mello et al., 2009; Huang et al., 2018; Paouri and Georgopoulos, 2019). In both sexes, plasma IL17A levels were significantly higher in MIA compared to C mice [p < 0.01 for each sex following Tukey's test, condition ×

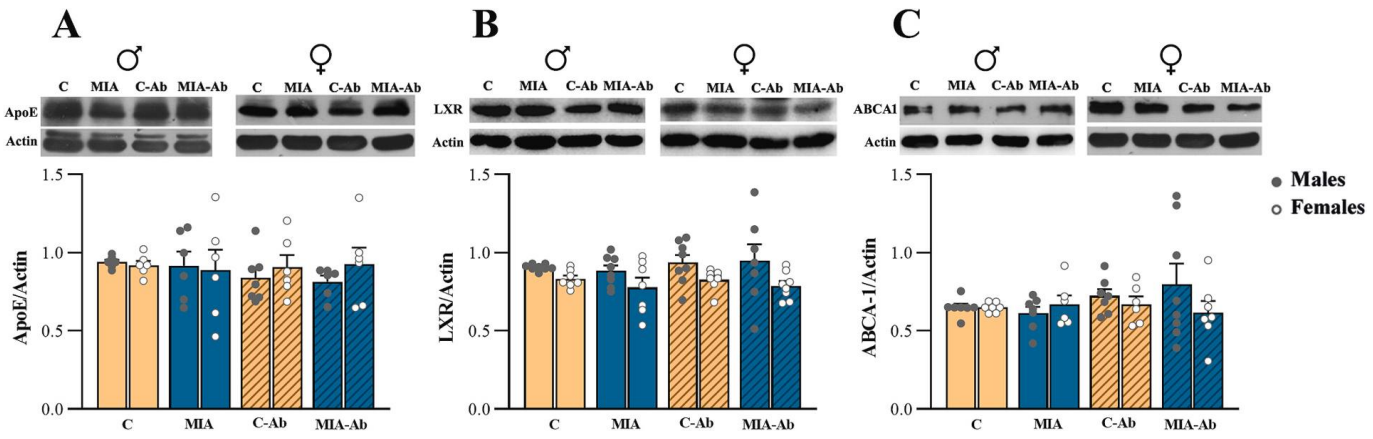

Fig. 5. Markers of cholesterol homeostasis. Apolipoprotein E (ApoE; A), liver X receptor (LXR; B), ABC Transporter A1 (ABCA-1; C) (with representative blots, normalized to controls) in the hippocampus from offspring prenatally treated with (C) saline/isotype control, (MIA) Poly(I:C)/isotype control, (C-Ab) saline/ anti-IL17A, or (MIA-Ab) Poly(I:C)/anti-IL17A are shown. Data are presented as mean + SEM, with individual data points shown as dots; n = 6–8 per group/sex.

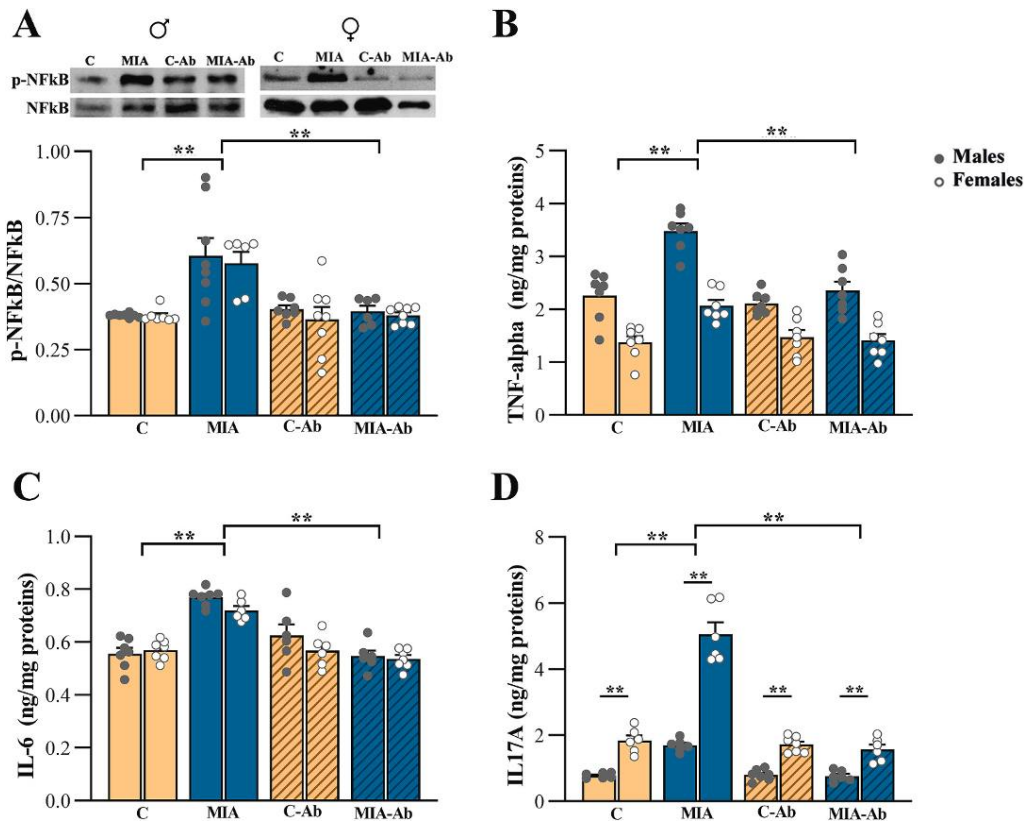

Fig. 6. NFkB pathway activation. Phosphorylated NFkB/NFkB ratio (protein content with representative blots, normalized to controls; A), concentrations of tumor necrosis factor alpha (TNF-alpha; B), interleukin 6 (IL-6; C), and interleukin 17A (IL17A; D), in the hippocampus from offspring prenatally treated with (C) saline/isotype control, (MIA) Poly(I:C)/isotype control, (C-Ab) saline/anti-IL17A, or (MIA-Ab) Poly(I:C)/anti-IL17A are shown. Data are presented as mean + SEM, with individual data points shown as dots; n = 6–8 per group/sex. **p < 0.001 (Three-way ANOVA followed by Tukey's post-hoc test).

treatment × sex interaction, F (1,41) = 20.80, p < 0.0001, Fig. 9A], with anti-IL17A preventing the cytokine increase in MIA offspring [p < 0.01 for each sex following Tukey's test]. Interestingly, while females exhibited significantly higher IL17A levels than males under control conditions [p < 0.05 following Tukey's test], in line with data described in humans (Binayke et al., 2025; Blanco et al., 2013; Guerrero-Garcia Jde et al., 2016; Newcomb et al., 2015; Sankaran-Walters et al., 2013), these sex-specific differences were no longer detectable following MIA. Notably, anti-IL17A treatment normalized cytokine levels and effectively restored the physiological sexual dimorphism [p < 0.01 following Tukey's test].

To provide a broader characterization of the systemic inflammatory status of MIA offspring, plasma levels of TNF-alpha and IL-6 were measured. Although no differences in plasma TNF-alpha levels between C and MIA groups were observed, significant sex differences were detected, with males exhibiting higher levels than females [main effect of sex, F (1,49) = 68.68, p < 0.0001, Fig. 9B], in agreement with previous reports (Asai et al., 2001; Bernardi et al., 2020; Yuan et al., 2015).

Finally, although IL-6 concentrations did not differ between C and MIA groups, they were significantly decreased by anti-IL17A [main effect of treatment, F (1, 45) = 22.68, p < 0.0001, Fig. 9C], particularly in females [p < 0.01 vs. isotype-treated females and anti-IL17A –treated males following Tukey's test, treatment × sex interaction F (1,45) = 3.459, p = 0.0694].

3.7. Associations between selected behavioral and molecular indexes

To gain insights into the potential involvement of early molecular changes in the observed behavioral phenotype, correlation analyses were performed between self-grooming duration in the social encounter with a sex- and age-matched conspecific and relevant molecular measures at the same developmental stage. Significant correlations were observed with levels of the proinflammatory cytokines IL-6 and IL17A, the neurotrophin BDNF, and the postsynaptic protein PSD-95 (Supplementary Fig. 5A-B). In males, self-grooming was positively correlated with hippocampal IL-6 and IL17A levels (r = 0.56, p = 0.001; r = 0.42, p = 0.041, respectively), whereas it was negatively correlated with PSD-95 (r = -0.568, p = 0.001). In females, self-grooming was positively correlated with plasma IL-6 and IL17A levels (r = 0.557, p = 0.003; r = 0.663, p = 0.001, respectively). In both sexes, self-grooming tended to be negatively correlated with BDNF (males: r = -0.348, p = 0.055; females: r = -0.366, p = 0.056). When attempting to investigate these associations within each experimental group and sex, no significant correlations were observed (Supplementary Tables 2 and 3).

4. Discussion

In this study, we mainly focused on the efficacy of anti-IL17A administration in preventing MIA-associated changes in key markers of synaptic function during early adolescence (PND 28) of male and female offspring, extending behavioral analysis from early infancy to late adolescence.

Here, we provide evidence that a single administration of anti-IL17A, delivered 24 h after MIA induction in pregnant mice, is sufficient to attenuate both early and long-lasting behavioral alterations induced by MIA. Atypical motor development is frequently reported in ASD individuals and often serves as an early indicator of this condition, as motor abnormalities typically precede the onset of social or cognitive impairments (Wilson et al., 2018). Consistently, we observed early and transient motor abnormalities in MIA-exposed male mice, characterized by hyperactivity and reduced motor control, neither of which was modulated by anti-IL17A treatment.

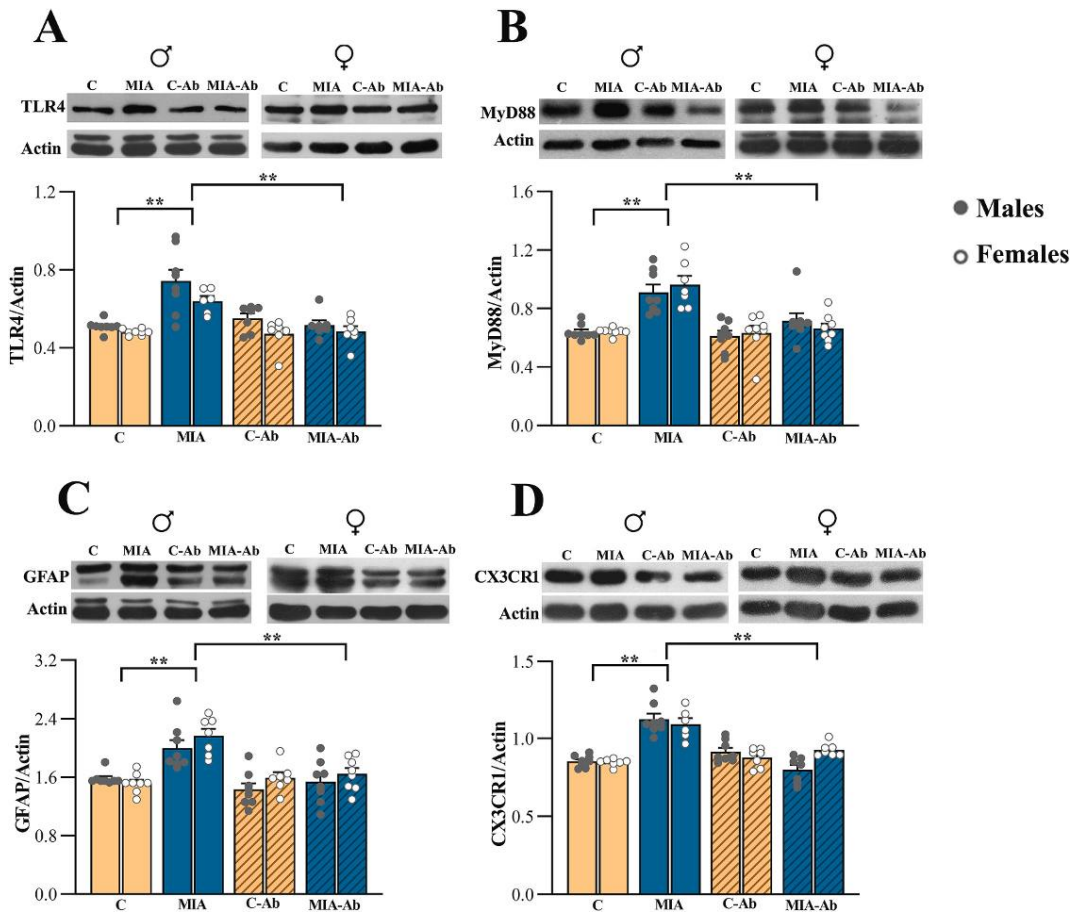

Fig. 7. Markers of neuroinflammation. Toll-like receptor 4 (TLR4; A), myeloid differentiation primary response 88 protein (MyD88; B), glial fibrillar acidic protein (GFAP; C), fractalkine receptor (CX3CR1; D). Representative blots (normalized to controls) in the hippocampus from offspring prenatally treated with (C) saline/isotype control, (MIA) Poly(I:C)/isotype control, (C-Ab) saline/anti-IL17A, or (MIA-Ab) Poly(I:C)/anti-IL17A are shown. Data are presented as mean + SEM, with individual data points shown as dots; n = 7–8 per group/sex. **p < 0.01 (Three-way ANOVA followed by Tukey's post-hoc test).

At early adolescence (PND 23), MIA-exposed animals did not display overt alterations in behavioral domains typically associated with ASD, such as repetitive behaviors and social approach deficits that emerged only at later ages between PND 35 and 59. Specifically, male MIA offspring exhibited increased self-grooming, indicative of repetitive behavior, whereas both sexes displayed no preference for interacting with a sex-matched social partner over an inanimate object. Remarkably, anti-IL17A treatment conferred a protective effect against these MIA-induced impairments. The sex differences in repetitive behaviors align with studies on BTBR mice, a validated mouse model of idiopathic autism (Amodeo et al., 2019; Bove et al., 2024), as well as in the MIA model itself (Ruskin et al., 2017; Xuan and Hampson, 2014) where male mice, but not females, displayed increased self-grooming despite comparable levels of social interaction. In our study, this elevated self-grooming was not paralleled by increased marble burying, another common measure of repetitive behavior. This dissociation, reported in other studies (Fernandez de Cossio et al., 2017; Sungur et al., 2014; Zanda et al., 2017), highlights limitations in their interchangeable use. Indeed, marble burying primarily reflects exploratory digging, encompassing both marble-oriented and displacement digging, without a clear habituation profile over time (Coppola et al., 2026; Thomas et al., 2009), whereas self-grooming is a self-directed behavior that more directly captures striatal dysfunction-driven repetitive patterns, as seen in ASD mouse models (Kalueff et al., 2016; Peca et al., 2011). Consistent with this distinction, we recently found no correlation between marble burying and self-grooming or other parameters of restricted and repetitive behaviors (Coppola et al., 2026).

Of note, we also observed subtle behavioral alterations (i.e., reduced self-grooming and social preference) in control offspring treated with anti-IL17A, specifically in males, potentially pointing to a role for IL17A signaling in physiological brain development. Consistent with this, Ribeiro et al., (2019) reported deficits in short-term memory and synaptic plasticity in mice lacking γδ T cells, a major source of IL17A in the brain meninges at steady state, or the IL17A cytokine itself (Ribeiro et al., 2019). Thus, IL17A might play a dual role, potentially beneficial under physiological conditions that warrants further investigation, but detrimental when excessively produced during inflammation, thereby contributing to neuroinflammatory pathogenesis and potentially to neurological and psychiatric disorders.

This study is the first, to our knowledge, to demonstrate that administration of anti-IL17A one day after MIA induction alleviates social deficits in offspring. In contrast, anti-IL17A administration two days after MIA induction has been reported to attenuate stereotyped behaviors without rescuing social impairments (Choi et al., 2016). The absence of an ASD-like behavioral phenotype at PND 23 is consistent with findings showing that animals at PND 28 still exhibited typical behavior, without ASD-like abnormalities (Dutra et al., 2023). Notably, in our study, 23-day-old MIA mice did not show increased self-grooming in an empty cage, but they displayed significantly elevated self-grooming upon exposure to a social stimulus. This behavioral pattern may indicate social discomfort and could potentially serve as an early indicator of subsequent impairments in social interaction. This evidence suggests that, at PND 28, ASD-like behavioral alterations induced by MIA have not yet fully manifested and prompted us to examine the

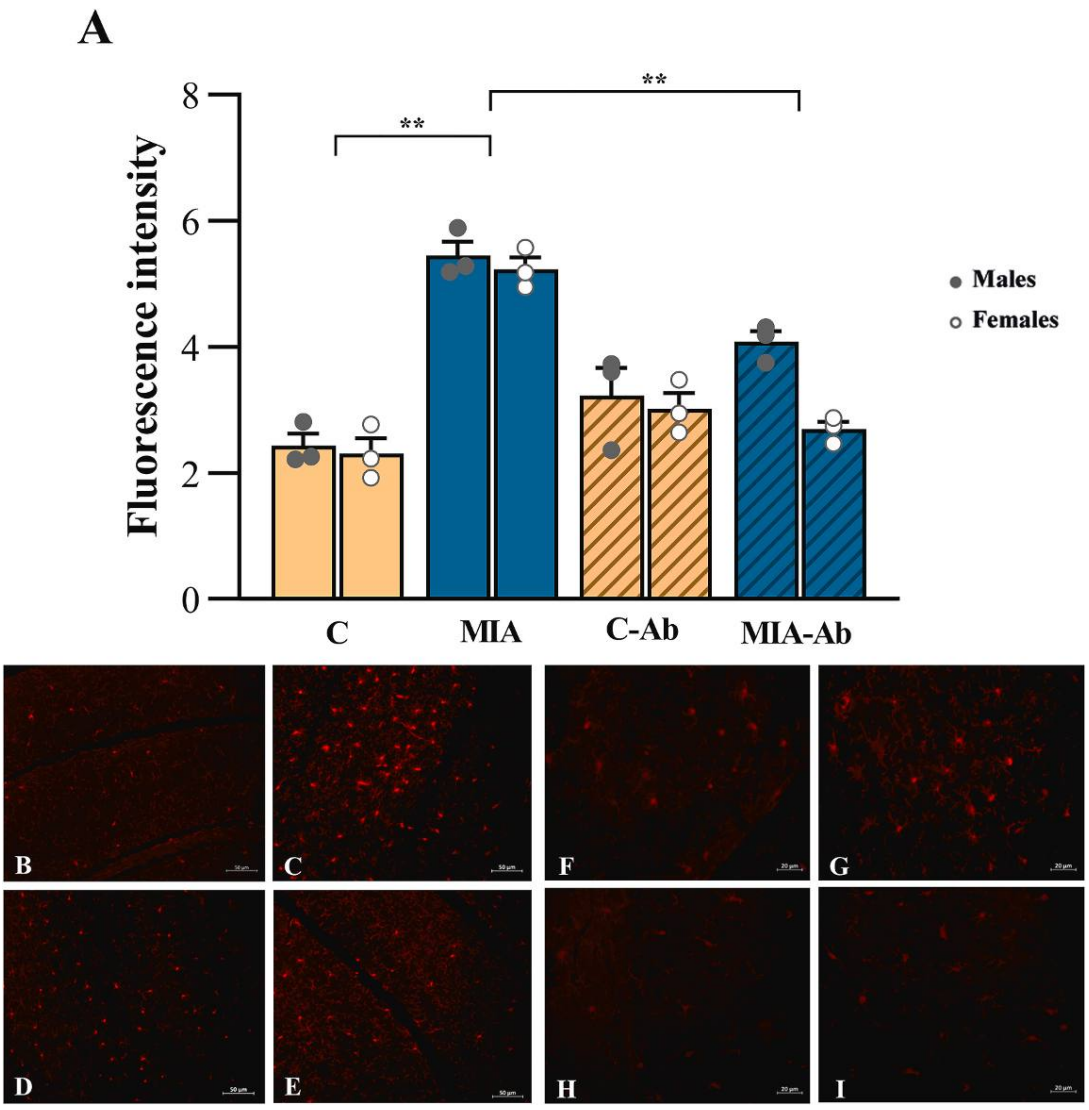

Fig. 8. Immunofluorescence for Iba1-positive cells. Iba-1 (A) relative fluorescence intensity in the hippocampus from offspring prenatally treated with (C) saline/isotype control, (MIA) Poly(I:C)/isotype control, (C-Ab) saline/anti-IL17A, or (MIA-Ab) Poly(I:C)/anti-IL17A is shown. Data are expressed as relative fluorescence intensity values (in arbitrary units). Each point represents mean + SEM from five photographic fields acquired at 20x magnification per each animal; n = 3 per group/sex; **p < 0.01 (Three-way ANOVA followed by Tukey's post-hoc test). B-I: representative images at fluorescence microscope showing the Iba-1 localization in C (B, males; F, females), MIA (C, males; G, females), C-Ab (D, males; H, females) and MIA-Ab (E, males; I, females).

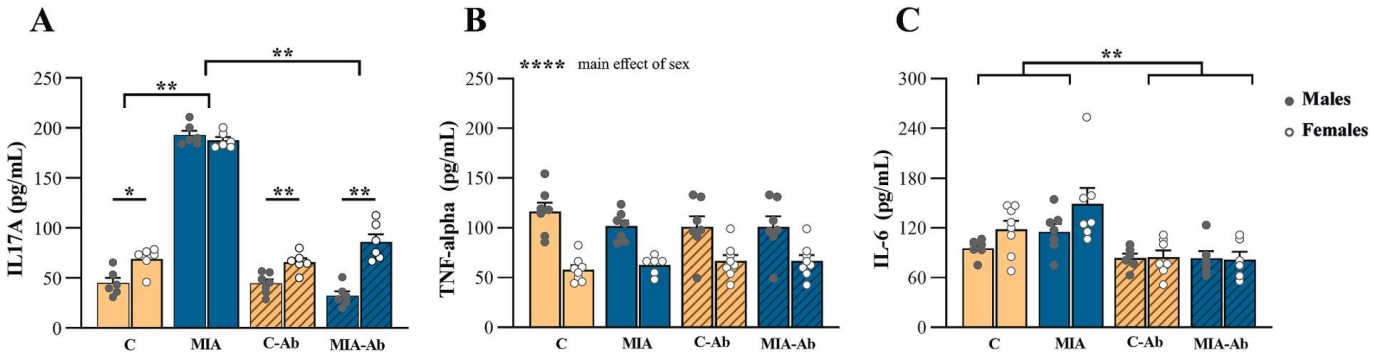

Fig. 9. Markers of systemic inflammation. Interleukin 17A (IL17A; A), tumor necrosis factor alpha (TNF-alpha; B) and interleukin 6 (IL-6; C) concentrations in the hippocampus from offspring prenatally treated with (C) saline/isotype control, (MIA) Poly(I:C)/isotype control, (C-Ab) saline/anti-IL17A, or (MIA-Ab) Poly(I:C)/anti-IL17A are shown. Data are presented as mean + SEM, with individual data points shown as dots; n = 6–7 per group/sex; *p < 0.05, **p < 0.01; ****p < 0.0001 (Three-way ANOVA followed by Tukey's post-hoc test).

molecular mechanisms underlying this latent phase, with a particular focus on neuroimmune and synaptic pathways. In this context, it should

be mentioned that the peripheral concentration of BDNF, a pivotal neurotrophin for neuroprotection, neurotransmitter modulation, and synaptic plasticity (Barde, 2025), has been proposed as a potential diagnostic marker of ASD, although several studies reported reduced serum levels in ASD subjects (Francis et al., 2018; Hashimoto et al., 2006; Kasarpalkar et al., 2014; Taurines et al., 2014), while others reported increased levels (Barbosa et al., 2020; Bryn et al., 2015; Ricci et al., 2013; Zheng et al., 2016). Our data show that MIA was associated with decreased hippocampal levels of mature BDNF in offspring of both sexes, consistent with previous findings (Dutra et al., 2023; Giovanoli et al., 2015; Tartaglione et al., 2022). In line, decreased expression of both GluN2B-containing NMDA-R, which plays a critical role in synaptic plasticity and neurodevelopment (Ge and Wang, 2023; Paoletti et al., 2013), and key proteins involved in synaptic plasticity, including SNAP-25, synaptotagmin, and PSD-95 was found (Giovanoli et al., 2016; Khalil et al., 2013) in the MIA model. Notably, prenatal anti-IL17A treatment prevented all hippocampal synaptic alterations in MIA offspring. The efficacy of the anti-IL17A could rely on attenuating MIA-induced neuroinflammation, characterized by elevated inflammatory mediators, such as IL17A, increased astrogliosis (higher GFAP expression), and enhanced microglial activation (higher number of Iba1-positive cells). Consistent with previous evidence (Talukdar et al., 2021), we found higher amount of both TLR4 and its downstream effector MyD88 in MIA offspring. Hence, it can be hypothesized that the activation of TLR4 pathway contributes to further fuel neuroinflammation in a positive loop, by potentiating NFkB signalling and microglial cells activation. Microglia is critically involved in physiological brain development, particularly in the process of synaptic pruning and plasticity (Gunner et al., 2019; Paolicelli et al., 2011; Schafer et al., 2012; Tremblay et al., 2011; Weinhard et al., 2018), and this task is achieved in part via the chemokine fractalkine, which binds to microglial fractalkine receptor CX3CR1 (Paolicelli et al., 2014; Wolf et al., 2013). The finding of CX3CR1 protein upregulation suggests a MIA-induced fractalkine signaling perturbation, which is fully prevented by IL17A blockade. CX3CR1-dependent pathway represents a major form of neuron-microglia communication, crucial for limiting microglia activation and allowing correct neurogenesis and network formation (Mecca et al., 2018). In this context, increased CX3CR1 correlated with neurobehavioral impairment and microglia dysregulation (Duarte-Campos et al., 2024; Lebovitz et al., 2019). In our model, CX3CR1 overexpression is associated with decreased levels of synaptic proteins supporting an early impairment of synaptic status in MIA offspring. Consistently, neuroinflammation has been shown to exert deleterious effects on hippocampus neurogenesis and function, particularly at synaptic level (Andoh et al., 2019; Chugh et al., 2013; de Bartolomeis et al., 2022). Since CX3CR1 expression can be increased by NFkB signaling (Chandrasekar et al., 2003), the neuroinflammatory condition observed in MIA offspring could be potentiated by the alteration of CX3CR1 signaling.

Our finding of increased hippocampal IL17A in MIA offspring is consistent with previous evidence from MIA models (Choi et al., 2016; Fan et al., 2024; Gillespie et al., 2024; Wang et al., 2025), while the reduction of IL17A following anti-IL17A supports the efficacy of the preventive strategy proposed in our study.

Of note, no behavioral changes have been observed in the early adolescent cohort, except for increased self-grooming during social interaction. In such perspective, self-grooming duration during the social encounter was correlated with relevant molecular markers to obtain a preliminary indication of their involvement in the behavioral phenotype at this developmental stage. Significant correlations emerged between self-grooming and IL-6, IL17A, BDNF, and PSD-95. Previous studies highlighted that IL-6 may influence neurodevelopment by altering glutamatergic synapse formation and signaling (Mirabella et al., 2021) while BDNF and PSD-95 are key mediators of synaptic maturation and plasticity, whose reduction has been linked to social deficits in ASD mouse models, including MIA (Coley and Gao, 2019; Scattoni et al., 2013; Tartaglione et al., 2022). Together, these data suggest that even subtle behavioral changes may reflect underlying neuroimmune and synaptic disturbances triggered by MIA.

Notably, hippocampal neuroinflammation and microglia activation here observed could result in the disruption of cellular proteostasis (Pintado et al., 2017; Sonninen et al., 2020), which is known to trigger aging (Lopez-Otin et al., 2013) and has been linked to the pathogenesis of neurodevelopmental disorders (Winden et al., 2025). Further, hippocampal dysfunction could also impair the hypothalamic pituitary adrenal (HPA) axis (Buchanan et al., 2004; Buchanan et al., 2009; Cole et al., 2022; McKeon et al., 2022; Semple et al., 2013; Winden et al., 2025), resulting in dysregulation of immune system and/or reproductive function (Bellavance and Rivest, 2014; Joseph and Whirledge, 2017; Nunez et al., 2025; Sorrells et al., 2009).

Furthermore, the lack of prominent behavioral and molecular sex differences following MIA in our study may reflect the developmental stages examined (early to late adolescence), as sex-specific effects often emerge later in adulthood (Gillespie et al., 2024; Hui et al., 2020; Yotova et al., 2024), possibly due to epigenetic and hormonal regulation (Gegenhuber et al., 2022; McCarthy and Nugent, 2013). Moreover, while we focused on ASD-like phenotypes, MIA has also been associated to deficits in sensorimotor gating, cognitive flexibility, and depressive-like behaviors, here not investigated, with sex differences reported in some studies (Gogos et al., 2020; Liu et al., 2024; Yotova et al., 2024), but not in others (Potter et al., 2025; Sal-Sarria et al., 2024; Schaer et al., 2025; Tartaglione et al., 2022). Importantly, the analysis of glutamatergic and dopaminergic pathways, reported as altered in MIA offspring, may unmask sex-specific differences, though most studies are male-biased (Amodeo et al., 2019; De Felice et al., 2019; Luchicchi et al., 2016; Mirabella et al., 2021; Nakamura et al., 2022; Santoni et al., 2023).

Alteration of brain cholesterol metabolism was previously suggested as a possible molecular mechanism underlying ASD, particularly through lipid raft disarrangements and consequent synaptic dysfunction (Buchovecky et al., 2013; Wang, 2014). However, here hippocampal levels of key players of cholesterol homeostasis were unaffected by MIA, supporting the hypothesis that aberrant cholesterol metabolism may not exist in all experimental models of ASD (Wang, 2014).

It should be mentioned that, differently from IL17A, plasma levels of TNF-alpha and IL-6, further markers of systemic inflammation, were not increased in MIA offspring of both sexes, thus suggesting that the imprint on the offspring's brains induced by Poly(I:C) treatment is mainly caused by IL17A signaling and not further fueled by circulating TNF-alpha and IL-6. This finding is supported by previous studies showing that Poly(I:C) administration, particularly during mid-gestation, does not affect plasma cytokines levels in offspring (Hameete et al., 2021).

One limitation of our study is that the anti-IL17A intervention was administered at a single time point (24 h post-MIA), which limits conclusions regarding the optimal window for preventive interventions. In addition, our analyses primarily focused on the hippocampus, whereas other brain regions such as prefrontal cortex, striatum, and cerebellum might also contribute to the behavioral changes observed and could be affected by MIA and IL17A blockade. Indeed, structural and functional neuronal alterations, in terms of impaired synaptic function and plasticity, have been described in MIA models beyond the hippocampus, also in the cortex and the cerebellum, where altered innervation of dendritic spines has been reported (Bergdolt and Dunaevsky, 2019).

Overall, our findings represent a mechanistic proof-of-concept of the role played by IL17A and indicate that early IL17A pathway blockade may offer a potential for preventing neurodevelopmental abnormalities associated with MIA, including behavioral deficits, neuroinflammation, and synaptic alterations. Highlighting the interplay between cytokine signaling and synaptic plasticity mechanisms, we provide a potential mechanistic link between early immune challenges and subsequent neurobehavioral alterations. Specifically, this study supports IL17A as a

promising target for modulating dysregulated neuroimmune mechanism, underscoring the importance of exploring new pharmacological or nutraceutical strategies targeting these pathways to ultimately improve ASD core symptoms.

CRediT authorship contribution statement

Maria Stefania Spagnuolo: Writing – review & editing, Writing – original draft, Visualization, Validation, Methodology, Investigation, Formal analysis, Data curation. **Giorgia Macchioni:** Writing – review & editing, Writing – original draft, Visualization, Validation, Methodology, Investigation, Formal analysis, Data curation. **Natasha Petecca:** Investigation. **Giulia Petruccioli:** Investigation. **Mattia De Magistris:** Investigation. **Francesca De Palma:** Investigation. **Marina Prisco:** Writing – review & editing, Methodology, Investigation. **Chiara Cipriani:** Writing – review & editing. **Martina Siracusano:** Writing – review & editing. **Gemma Calamandrei:** Writing – review & editing. **Laura Ricceri:** Writing – review & editing. **Luisa Cigliano:** Writing – review & editing, Writing – original draft, Validation, Supervision, Resources, Project administration, Investigation, Funding acquisition, Conceptualization. **Anna Maria Tartaglione:** Writing – review & editing, Writing – original draft, Validation, Supervision, Resources, Project administration, Investigation, Funding acquisition, Conceptualization.

Funding

This work was supported by grants from: i) Italian Ministry of Health [grant number GR-2021-12372680 to AMT]; ii) University of Naples Federico II—Ricerca Dip 2023/2024 to LC; iii) National Recovery and Resilience Plan, mission 4, Component C2, funded by the European Union – NextGenerationEU, PRIN 2022PNRR (P2022LTFLR) to LC.

Declaration of competing interest

The authors declare that they have no known competing financial interests or personal relationships that could have appeared to influence the work reported in this paper.

Acknowledgments

We thank Irene Coppola and Raffaele Ascione for their support with the *in vivo* and *ex vivo* studies, respectively, and Luigia Cancemi for animal care.

Appendix A. Supplementary data

Supplementary data to this article can be found online at https://doi.org/10.1016/j.bbi.2026.106820.

Data availability

Data will be made available on request.

References

Amodeo, D.A., Pahua, A.E., Zarate, M., Taylor, J.A., Peterson, S., Posadas, R., Oliver, B. L., Amodeo, L.R., 2019. Differences in the expression of restricted repetitive behaviors in female and male BTBR T + tf/J mice. Behav. Brain Res. 372, 112028.

Andoh, M., Shibata, K., Okamoto, K., Onodera, J., Morishita, K., Miura, Y., Ikegaya, Y., Koyama, R., 2019. Exercise reverses behavioral and synaptic abnormalities after maternal inflammation. Cell Rep. 27 (2817–2825), e2815.

Arrode-Bruses, G., Bruses, J.L., 2012. Maternal immune activation by poly I:C induces expression of cytokines IL-1beta and IL-13, chemokine MCP-1 and colony stimulating factor VEGF in fetal mouse brain. J. Neuroinflammation 9, 83.

Asai, K., Hiki, N., Mimura, Y., Ogawa, T., Unou, K., Kaminishi, M., 2001. Gender differences in cytokine secretion by human peripheral blood mononuclear cells: role of estrogen in modulating LPS-induced cytokine secretion in an ex vivo septic model. Shock 16, 340–343.

American Psychiatric Association, 2013. Diagnostic and statistical manual of mental disorders (5th ed.).

Barbosa, A.G., Pratesi, R., Paz, G.S.C., Dos Santos, M., Uenishi, R.H., Nakano, E.Y., Gandolfi, L., Pratesi, C.B., 2020. Assessment of BDNF serum levels as a diagnostic marker in children with autism spectrum disorder. Sci. Rep. 10, 17348.

Barde, Y.A., 2025. The physiopathology of brain-derived neurotrophic factor. Physiol. Rev. 105, 2073–2140.

Bellavance, M.A., Rivest, S., 2014. The HPA - immune axis and the immunomodulatory actions of glucocorticoids in the brain. Front. Immunol. 5, 136.

Bergdolt, L., Dunaevsky, A., 2019. Brain changes in a maternal immune activation model of neurodevelopmental brain disorders. Prog. Neurobiol. 175, 1–19.

Bernardi, S., Toffoli, B., Tonon, F., Francica, M., Campagnolo, E., Ferretti, T., Comar, S., Giudici, F., Stenner, E., Fabris, B., 2020. Sex Differences in Proatherogenic Cytokine Levels. International journal of molecular sciences 21.

Binayke, A., Dalal, R., Suri, C., Dandotiya, J., Sadhu, S., Kumar, Y., Asthana, S., Rathore, D.K., Awasthi, A., 2025. Testosterone Suppresses IL-17 Expression by Targeting RORgammat Functions. Eur. J. Immunol. 55, e70016.

Blanco, L.P., Plegue, M., Fung-Leung, W.P., Holoshitz, J., 2013. Gender-biased regulation of human IL-17-producing cells in vitro by peptides corresponding to distinct HLA-DRB1 allele-coded sequences. J Immune Based Ther Vaccines Antimicrob 2, 29–38.

Bove, M., Sikora, V., Santoro, M., Agosti, L.P., Palmieri, M.A., Dimonte, S., Tucci, P., Schiavone, S., Morgese, M.G., Trabace, L., 2024. Sex differences in the BTBR idiopathic mouse model of autism spectrum disorders: Behavioural and redox-related hippocampal alterations. Neuropharmacology 260, 110134.

Brown, A.S., Meyer, U., 2018. Maternal immune activation and neuropsychiatric illness: a translational research perspective. Am. J. Psychiatry 175, 1073–1083.

Bryn, V., Halvorsen, B., Ueland, T., Isaksen, J., Kolkova, K., Ravn, K., Skjeldal, O.H., 2015. Brain derived neurotrophic factor (BDNF) and autism spectrum disorders (ASD) in childhood. Eur. J. Paediatr. Neurol. 19, 411–414.

Buchanan, T.W., Kern, S., Allen, J.S., Tranel, D., Kirschbaum, C., 2004. Circadian regulation of cortisol after hippocampal damage in humans. Biol. Psychiatry 56, 651–656.

Buchanan, T.W., Tranel, D., Kirschbaum, C., 2009. Hippocampal damage abolishes the cortisol response to psychosocial stress in humans. Horm. Behav. 56, 44–50.

Buchovecky, C.M., Turley, S.D., Brown, H.M., Kyle, S.M., McDonald, J.G., Liu, B., Pieper, A.A., Huang, W., Katz, D.M., Russell, D.W., Shendure, J., Justice, M.J., 2013. A suppressor screen in Mecp2 mutant mice implicates cholesterol metabolism in Rett syndrome. Nat. Genet. 45, 1013–1020.

Cartocci, V., Catallo, M., Tempestilli, M., Segatto, M., Pfrieger, F.W., Bronzuoli, M.R., Scuderi, C., Servadio, M., Trezza, V., Pallottini, V., 2018. Altered brain cholesterol/isoprenoid metabolism in a rat model of autism spectrum disorders. Neuroscience 372, 27–37.

Cartocci, V., Tonini, C., Di Pippo, T., Vuono, F., Schiavi, S., Marino, M., Trezza, V., Pallottini, V., 2019. Prenatal exposure to valproate induces sex-, age-, and tissue-dependent alterations of cholesterol metabolism: potential implications on autism. J. Cell. Physiol. 234, 4362–4374.

Chandrasekar, B., Mummidi, S., Perla, R.P., Bysani, S., Dulin, N.O., Liu, F., Melby, P.C., 2003. Fractalkine (CX3CL1) stimulated by nuclear factor kappaB (NF-kappaB)-dependent inflammatory signals induces aortic smooth muscle cell proliferation through an autocrine pathway. Biochem. J. 373, 547–558.

Choi, G.B., Yim, Y.S., Wong, H., Kim, S., Kim, H., Kim, S.V., Hoeffer, C.A., Littman, D.R., Huh, J.R., 2016. The maternal interleukin-17a pathway in mice promotes autism-like phenotypes in offspring. Science 351, 933–939.

Chugh, D., Nilsson, P., Afjei, S.A., Bakochi, A., Ekdahl, C.T., 2013. Brain inflammation induces post-synaptic changes during early synapse formation in adult-born hippocampal neurons. Exp. Neurol. 250, 176–188.

Cipriani, C., Tartaglione, A.M., Giudice, M., D'Avorio, E., Petrone, V., Toschi, N., Chiarotti, F., Miele, M.T., Calamandrei, G., Garaci, E., Matteucci, C., Sinibaldi-Vallebona, P., Ricceri, L., Balestrieri, E., 2022. Differential Expression of Endogenous Retroviruses and Inflammatory Mediators in Female and Male Offspring in a Mouse Model of Maternal Immune Activation. International journal of molecular sciences 23.

Coffey, K.R., Marx, R.E., Neumaier, J.F., 2019. DeepSqueak: a deep learning-based system for detection and analysis of ultrasonic vocalizations. Neuropsychopharmacology : Official Publication of the American College of Neuropsychopharmacology 44, 859–868.

Cole, A.B., Montgomery, K., Bale, T.L., Thompson, S.M., 2022. What the hippocampus tells the HPA axis: Hippocampal output attenuates acute stress responses via disynaptic inhibition of CRF+ PVN neurons. Neurobiol. Stress 20, 100473.

Coley, A.A., Gao, W.J., 2019. PSD-95 deficiency disrupts PFC-associated function and behavior during neurodevelopment. Sci. Rep. 9, 9486.

Coppola, I., De Magistris, M., Macchioni, G., Calamandrei, G., Ricceri, L., Tartaglione, A. M., 2026. Beyond marbles buried: a multidimensional analysis of the marble burying test in the C57BL/6J mouse strain. Behav. Brain Res. 497, 115888.

Courtney, R., Landreth, G.E., 2016. LXR regulation of brain cholesterol: from development to disease. Trends Endocrinol Metab 27, 404–414.

D'Mello, C., Le, T., Swain, M.G., 2009. Cerebral microglia recruit monocytes into the brain in response to tumor necrosis factoralpha signaling during peripheral organ inflammation. J. Neurosci. 29, 2089–2102.

de Bartolomeis, A., Barone, A., Vellucci, L., Mazza, B., Austin, M.C., Iasevoli, F., Ciccarelli, M., 2022. Linking inflammation, aberrant glutamate-dopamine interaction, and post-synaptic changes: translational relevance for schizophrenia and antipsychotic treatment: a systematic review. Mol. Neurobiol. 59, 6460–6501.

De Felice, M., Melis, M., Aroni, S., Muntoni, A.L., Fanni, S., Frau, R., Devoto, P., Pistis, M., 2019. The PPARalpha agonist fenofibrate attenuates disruption of

dopamine function in a maternal immune activation rat model of schizophrenia. CNS Neurosci. Ther. 25, 549–561.
Duarte-Campos, J.F., Vazquez-Moreno, C.N., Martinez-Marcial, M., Chavarria, A., Ramirez-Carreto, R.J., Velasco Velazquez, M.A., De La Fuente-Granada, M., Gonzalez-Arenas, A., 2024. Changes in neuroinflammatory markers and microglial density in the hippocampus and prefrontal cortex of the C58/J mouse model of autism. Eur. J. Neurosci. 59, 154–173.
Dutra, M.L., Dias, P., Freiberger, V., Ventura, L., Comim, C.M., Martins, D.F., Bobinski, F., 2023. Maternal immune activation induces autism-like behavior and reduces brain-derived neurotrophic factor levels in the hippocampus and offspring cortex of C57BL/6 mice. Neurosci. Lett. 793, 136974.
Fan, L., Zeng, X., Jiang, Y., Zheng, D., Wang, H., Qin, Q., Li, M., Wang, H., Liu, H., Liang, S., Pang, X., Shi, S., Wu, L., Liang, S., 2024. Yigansan ameliorates maternal immune activation-induced autism-like behaviours by regulating the IL-17A/TRAF6/MMP9 pathway: Network analysis and experimental validation. Phytomedicine 128, 155386.
Fernandez de Cossio, L., Guzman, A., van der Veldt, S., Luheshi, G.N., 2017. Prenatal infection leads to ASD-like behavior and altered synaptic pruning in the mouse offspring. Brain Behav. Immun. 63, 88–98.
Filipello, F., Morini, R., Corradini, I., Zerbi, V., Canzi, A., Michalski, B., Erreni, M., Markicevic, M., Starvaggi-Cucuzza, C., Otero, K., Piccio, L., Cignarella, F., Perrucci, F., Tamborini, M., Genua, M., Rajendran, L., Menna, E., Vetrano, S., Fahnestock, M., Paolicelli, R.C., Matteoli, M., 2018. The microglial innate immune receptor TREM2 is required for synapse elimination and normal brain connectivity. Immunity 48 (979–991), e978.
Francis, K., Dougali, A., Sideri, K., Kroupis, C., Vasdekis, V., Dima, K., Douzenis, A., 2018. Brain-derived neurotrophic factor (BDNF) in children with ASD and their parents: a 3-year follow-up. Acta Psychiatr. Scand. 137, 433–441.
Garay, P.A., Hsiao, E.Y., Patterson, P.H., McAllister, A.K., 2013. Maternal immune activation causes age- and region-specific changes in brain cytokines in offspring throughout development. Brain Behav. Immun. 31, 54–68.
Garcia-Valtanen, P., van Diermen, B.A., Lakhan, N., Lousberg, E.L., Robertson, S.A., Hayball, J.D., Diener, K.R., 2020. Maternal host responses to poly(I:C) during pregnancy leads to both dysfunctional immune profiles and altered behaviour in the offspring. Am. J. Reprod. Immunol. 84, e13260.
Ge, Y., Wang, Y.T., 2023. GluN2B-containing NMDARs in the mammalian brain: pharmacology, physiology, and pathology. Front. Mol. Neurosci. 16, 1190324.
Gegenhuber, B., Wu, M.V., Bronstein, R., Tollkuhn, J., 2022. Gene regulation by gonadal hormone receptors underlies brain sex differences. Nature 606, 153–159.
Gilbert, J., Man, H.Y., 2017. Fundamental elements in autism: from neurogenesis and neurite growth to synaptic plasticity. Front. Cell. Neurosci. 11, 359.
Gillespie, B., Houghton, M.J., Ganio, K., McDevitt, C.A., Bennett, D., Dunn, A., Raju, S., Schroeder, A., Hill, R.A., Cardoso, B.R., 2024. Maternal selenium dietary supplementation alters sociability and reinforcement learning deficits induced by in utero exposure to maternal immune activation in mice. Brain Behav. Immun. 116, 349–361.
Giovanoli, S., Notter, T., Richetto, J., Labouesse, M.A., Vuillermot, S., Riva, M.A., Meyer, U., 2015. Late prenatal immune activation causes hippocampal deficits in the absence of persistent inflammation across aging. J. Neuroinflammation 12, 221.
Giovanoli, S., Weber-Stadlbauer, U., Schedlowski, M., Meyer, U., Engler, H., 2016. Prenatal immune activation causes hippocampal synaptic deficits in the absence of overt microglia anomalies. Brain Behav. Immun. 55, 25–38.
Gogos, A., Sbisa, A., Witkamp, D., van den Buuse, M., 2020. Sex differences in the effect of maternal immune activation on cognitive and psychosis-like behaviour in long evans rats. Eur. J. Neurosci. 52, 2614–2626.
Guerrero-Garcia Jde, J., Castaneda-Moreno, V.A., Torres-Carrillo, N., Munoz-Valle, J.F., Bitzer-Quintero, O.K., Ponce-Regalado, M.D., Mireles-Ramirez, M.A., Valle, Y., Ortuno-Sahagun, D., 2016. Interleukin-17A levels vary in relapsing-remitting multiple sclerosis patients in association with their age, treatment and the time of evolution of the disease. Neuroimmunomodulation 23, 8–17.
Gunner, G., Cheadle, L., Johnson, K.M., Ayata, P., Badimon, A., Mondo, E., Nagy, M.A., Liu, L., Bemiller, S.M., Kim, K.W., Lira, S.A., Lamb, B.T., Tapper, A.R., Ransohoff, R. M., Greenberg, M.E., Schaefer, A., Schafer, D.P., 2019. Sensory lesioning induces microglial synapse elimination via ADAM10 and fractalkine signaling. Nat. Neurosci. 22, 1075–1088.
Haddad, F.L., Lu, L., Baines, K.J., Schmid, S., 2020. Sensory filtering disruption caused by poly I:C - timing of exposure and other experimental considerations. Brain, Behavior, & Immunity - Health 9, 100156.
Hameete, B.C., Fernandez-Calleja, J.M.S., de Groot, M., Oppewal, T.R., Tiemessen, M.M., Hogenkamp, A., de Vries, R.B.M., Groenink, L., 2021. The poly(I:C)-induced maternal immune activation model; a systematic review and meta-analysis of cytokine levels in the offspring. Brain, Behavior, & Immunity - Health 11, 100192.
Hashimoto, K., Iwata, Y., Nakamura, K., Tsujii, M., Tsuchiya, K.J., Sekine, Y., Suzuki, K., Minabe, Y., Takei, N., Iyo, M., Mori, N., 2006. Reduced serum levels of brain-derived neurotrophic factor in adult male patients with autism. Prog. Neuropsychopharmacol. Biol. Psychiatry 30, 1529–1531.
Huang, C., Irwin, M.G., Wong, G.T.C., Chang, R.C.C., 2018. Evidence of the impact of systemic inflammation on neuroinflammation from a non-bacterial endotoxin animal model. J. Neuroinflammation 15, 147.
Hui, C.W., Vecchiarelli, H.A., Gervais, E., Luo, X., Michaud, F., Scheefhals, L., Bisht, K., Sharma, K., Topolnik, L., Tremblay, M.E., 2020. Sex differences of microglia and synapses in the hippocampal dentate gyrus of adult mouse offspring exposed to maternal immune activation. Front. Cell. Neurosci. 14, 558181.
Ito, H.T., Smith, S.E., Hsiao, E., Patterson, P.H., 2010. Maternal immune activation alters nonspatial information processing in the hippocampus of the adult offspring. Brain Behav. Immun. 24, 930–941.
Jiang, H.Y., Xu, L.L., Shao, L., Xia, R.M., Yu, Z.H., Ling, Z.X., Yang, F., Deng, M., Ruan, B., 2016. Maternal infection during pregnancy and risk of autism spectrum disorders: a systematic review and meta-analysis. Brain Behav. Immun. 58, 165–172.
Joseph, D.N., Whirledge, S., 2017. Stress and the HPA Axis: Balancing Homeostasis and Fertility. International journal of molecular sciences 18.
Kalueff, A.V., Stewart, A.M., Song, C., Berridge, K.C., Graybiel, A.M., Fentress, J.C., 2016. Neurobiology of rodent self-grooming and its value for translational neuroscience. Nat. Rev. Neurosci. 17, 45–59.
Kasarpalkar, N.J., Kothari, S.T., Dave, U.P., 2014. Brain-Derived Neurotrophic Factor in children with Autism Spectrum Disorder. Ann. Neurosci. 21, 129–133.
Keith, R.E., Azcarate, J.M., Keith, M.J., Hung, C.W., Badakhsh, M.F., Dumas, T.C., 2019. Direct Intracellular Signaling by the Carboxy terminus of NMDA Receptor GluN2 Subunits Regulates Dendritic Morphology in Hippocampal CA1 Pyramidal Neurons. Neuroscience 396, 138–153.
Khalil, O.S., Forrest, C.M., Pisar, M., Smith, R.A., Darlington, L.G., Stone, T.W., 2013. Prenatal activation of maternal TLR3 receptors by viral-mimetic poly(I:C) modifies GluN2B expression in embryos and sonic hedgehog in offspring in the absence of kynurenine pathway activation. Immunopharmacol. Immunotoxicol. 35, 581–593.
Kim, W.S., Rahmanto, A.S., Kamili, A., Rye, K.A., Guillemin, G.J., Gelissen, I.C., Jessup, W., Hill, A.F., Garner, B., 2007. Role of ABCG1 and ABCA1 in regulation of neuronal cholesterol efflux to apolipoprotein E discs and suppression of amyloid-beta peptide generation. J. Biol. Chem. 282, 2851–2861.
Kwon, H.K., Choi, G.B., Huh, J.R., 2022. Maternal inflammation and its ramifications on fetal neurodevelopment. Trends Immunol. 43, 230–244.
Lebovitz, Y., Kowalski, E.A., Wang, X., Kelly, C., Lee, M., McDonald, V., Ward, R., Creasey, M., Mills, W., Gudenschwager Basso, E.K., Hazy, A., Hrubec, T., Theus, M. H., 2019. Lactobacillus rescues postnatal neurobehavioral and microglial dysfunction in a model of maternal microbiome dysbiosis. Brain Behav. Immun. 81, 617–629.
Liu, Y., Hang, X., Zhang, Y., Fang, Y., Yuan, S., Zhang, Y., Wu, B., Kong, Y., Kuang, Z., Sun, W., 2024. Maternal immune activation induces sex-dependent behavioral differences in a rat model of schizophrenia. Front. Psych. 15, 1375999.
Lopez-Otin, C., Blasco, M.A., Partridge, L., Serrano, M., Kroemer, G., 2013. The hallmarks of aging. Cell 153, 1194–1217.
Luchicchi, A., Lecca, S., Melis, M., De Felice, M., Cadeddu, F., Frau, R., Muntoni, A.L., Fadda, P., Devoto, P., Pistis, M., 2016. Maternal Immune Activation Disrupts Dopamine System in the Offspring. Int. J. Neuropsychopharmacol. 19.
Malkova, N.V., Yu, C.Z., Hsiao, E.Y., Moore, M.J., Patterson, P.H., 2012. Maternal immune activation yields offspring displaying mouse versions of the three core symptoms of autism. Brain Behav. Immun. 26, 607–616.
McCarthy, M.M., Nugent, B.M., 2013. Epigenetic contributions to hormonally-mediated sexual differentiation of the brain. J. Neuroendocrinol. 25, 1133–1140.
McKeon, J.W., Torres, J., Kazama, A.M., Bachevalier, J., Raper, J., 2022. Differential responses toward conditioned and unconditioned stimuli, but decreased hypothalamic-pituitary-adrenal axis responsiveness in neonatal hippocampal lesioned monkeys. Dev. Cogn. Neurosci. 58, 101165.
Mecca, C., Giambanco, I., Donato, R., Arcuri, C., 2018. Microglia and Aging: The Role of the TREM2-DAP12 and CX3CL1-CX3CR1 Axes. International journal of molecular sciences 19.
Meyer, U., 2014. Prenatal poly(i:C) exposure and other developmental immune activation models in rodent systems. Biol. Psychiatry 75, 307–315.
Meyer, U., 2019. Neurodevelopmental Resilience and Susceptibility to Maternal Immune Activation. Trends Neurosci. 42, 793–806.
Meyer, U., Feldon, J., 2010. Epidemiology-driven neurodevelopmental animal models of schizophrenia. Prog. Neurobiol. 90, 285–326.
Meyer, U., Feldon, J., 2012. To poly(I:C) or not to poly(I:C): advancing preclinical schizophrenia research through the use of prenatal immune activation models. Neuropharmacology 62, 1308–1321.
Meyer, U., Feldon, J., Dammann, O., 2011. Schizophrenia and autism: both shared and disorder-specific pathogenesis via perinatal inflammation? Pediatr. Res. 69, 26R–33R.
Meyer, U., Feldon, J., Fatemi, S.H., 2009a. In-vivo rodent models for the experimental investigation of prenatal immune activation effects in neurodevelopmental brain disorders. Neurosci. Biobehav. Rev. 33, 1061–1079.
Meyer, U., Feldon, J., Yee, B.K., 2009b. A review of the fetal brain cytokine imbalance hypothesis of schizophrenia. Schizophr. Bull. 35, 959–972.
Meyer, U., Yee, B.K., Feldon, J., 2007. The neurodevelopmental impact of prenatal infections at different times of pregnancy: the earlier the worse? Neuroscientist 13, 241–256.
Milbocker, K.A., Campbell, T.S., Collins, N., Kim, S., Smith, E.A., Roth, T.L., Klintsova, A. Y., 2021. Glia-driven brain circuit refinement is altered by early-life adversity: behavioral outcomes. Front. Behav. Neurosci. 15, 786234.
Mirabella, F., Desiato, G., Mancinelli, S., Fossati, G., Rasile, M., Morini, R., Markicevic, M., Grimm, C., Amegandjin, C., Termanini, A., Peano, C., Kunderfranco, P., di Cristo, G., Zerbi, V., Menna, E., Lodato, S., Matteoli, M., Pozzi, D., 2021. Prenatal interleukin 6 elevation increases glutamatergic synapse density and disrupts hippocampal connectivity in offspring. Immunity 54 (2611–2631), e2618.
Nakamura, J.P., Schroeder, A., Gibbons, A., Sundram, S., Hill, R.A., 2022. Timing of maternal immune activation and sex influence schizophrenia-relevant cognitive constructs and neuregulin and GABAergic pathways. Brain Behav. Immun. 100, 70–82.
Newcomb, D.C., Cephus, J.Y., Boswell, M.G., Fahrenholz, J.M., Langley, E.W., Feldman, A.S., Zhou, W., Dulek, D.E., Goleniewska, K., Woodward, K.B., Sevin, C.M., Hamilton, R.G., Kolls, J.K., Peebles Jr., R.S., 2015. Estrogen and progesterone decrease let-7f microRNA expression and increase IL-23/IL-23 receptor signaling and

IL-17A production in patients with severe asthma. J. Allergy Clin. Immunol. 136 (1025–1034), e1011.
Nunez, S.G., Rabelo, S.P., Subotic, N., Caruso, J.W., Knezevic, N.N., 2025. Chronic Stress and Autoimmunity: The Role of HPA Axis and Cortisol Dysregulation. International journal of molecular sciences 26.
Oh-Nishi, A., Obayashi, S., Sugihara, I., Minamimoto, T., Suhara, T., 2010. Maternal immune activation by polyriboinosinic-polyribocytidilic acid injection produces synaptic dysfunction but not neuronal loss in the hippocampus of juvenile rat offspring. Brain Res. 1363, 170–179.
Osman, H.C., Moreno, R., Rose, D., Rowland, M.E., Ciernia, A.V., Ashwood, P., 2024. Impact of maternal immune activation and sex on placental and fetal brain cytokine and gene expression profiles in a preclinical model of neurodevelopmental disorders. J. Neuroinflammation 21, 118.
Page, N.F., Gandal, M.J., Estes, M.L., Cameron, S., Buth, J., Parhami, S., Ramaswami, G., Murray, K., Amaral, D.G., Van de Water, J.A., Schumann, C.M., Carter, C.S., Bauman, M.D., McAllister, A.K., Geschwind, D.H., 2021. Alterations in retrotransposition, synaptic connectivity, and myelination implicated by transcriptomic changes following maternal immune activation in nonhuman primates. Biol. Psychiatry 89, 896–910.
Paoletti, P., Bellone, C., Zhou, Q., 2013. NMDA receptor subunit diversity: impact on receptor properties, synaptic plasticity and disease. Nat. Rev. Neurosci. 14, 383–400.
Paolicelli, R.C., Bisht, K., Tremblay, M.E., 2014. Fractalkine regulation of microglial physiology and consequences on the brain and behavior. Front. Cell. Neurosci. 8, 129.
Paolicelli, R.C., Bolasco, G., Pagani, F., Maggi, L., Scianni, M., Panzanelli, P., Giustetto, M., Ferreira, T.A., Guiducci, E., Dumas, L., Ragozzino, D., Gross, C.T., 2011. Synaptic pruning by microglia is necessary for normal brain development. Science 333, 1456–1458.
Paouri, E., Georgopoulos, S., 2019. Systemic and CNS Inflammation Crosstalk: Implications for Alzheimer's Disease. Curr. Alzheimer Res. 16, 559–574.
Peca, J., Feliciano, C., Ting, J.T., Wang, W., Wells, M.F., Venkatraman, T.N., Lascola, C. D., Fu, Z., Feng, G., 2011. Shank3 mutant mice display autistic-like behaviours and striatal dysfunction. Nature 472, 437–442.
Pendyala, G., Chou, S., Jung, Y., Coiro, P., Spartz, E., Padmashri, R., Li, M., Dunaevsky, A., 2017. Maternal immune activation causes behavioral impairments and altered cerebellar cytokine and synaptic protein expression. Neuropsychopharmacology : Official Publication of the American College of Neuropsychopharmacology 42, 1435–1446.
Pfrieger, F.W., Ungerer, N., 2011. Cholesterol metabolism in neurons and astrocytes. Prog. Lipid Res. 50, 357–371.
Pintado, C., Macias, S., Dominguez-Martin, H., Castano, A., Ruano, D., 2017. Neuroinflammation alters cellular proteostasis by producing endoplasmic reticulum stress, autophagy activation and disrupting ERAD activation. Sci. Rep. 7, 8100.
Potter, H.G., Woods, R.M., Lorusso, J.M., Revill, G., Harte, M.K., Glazier, J.D., Neill, J.C., Hager, R., 2025. Prenatal poly(I:C) exposure, rather than altered maternal care, causes offspring behavioural and cognitive deficits in a rat model of neurodevelopmental disorders. Brain Behav. Immun. 129, 186–195.
Reiner, A., Levitz, J., 2018. Glutamatergic Signaling in the Central nervous System: Ionotropic and Metabotropic Receptors in Concert. Neuron 98, 1080–1098.
Ribeiro, M., Brigas, H.C., Temido-Ferreira, M., Pousinha, P.A., Regen, T., Santa, C., Coelho, J.E., Marques-Morgado, I., Valente, C.A., Omenetti, S., Stockinger, B., Waisman, A., Manadas, B., Lopes, L.V., Silva-Santos, B., Ribot, J.C., 2019. Meningeal gammadelta T cell-derived IL-17 controls synaptic plasticity and short-term memory. Sci. Immunol. 4.
Ricci, S., Businaro, R., Ippoliti, F., Lo Vasco, V.R., Massoni, F., Onofri, E., Troili, G.M., Pontecorvi, V., Morelli, M., Rapp Ricciardi, M., Archer, T., 2013. Altered cytokine and BDNF levels in autism spectrum disorder. Neurotox. Res. 24, 491–501.
Ruskin, D.N., Murphy, M.I., Slade, S.L., Masino, S.A., 2017. Ketogenic diet improves behaviors in a maternal immune activation model of autism spectrum disorder. PLoS One 12, e0171643.
Sal-Sarria, S., Conejo, N.M., Gonzalez-Pardo, H., 2024. Maternal immune activation and its multifaceted effects on learning and memory in rodent offspring: a systematic review. Neurosci. Biobehav. Rev. 164, 105844.
Sankaran-Walters, S., Macal, M., Grishina, I., Nagy, L., Goulart, L., Coolidge, K., Li, J., Fenton, A., Williams, T., Miller, M.K., Flamm, J., Prindiville, T., George, M., Dandekar, S., 2013. Sex differences matter in the gut: effect on mucosal immune activation and inflammation. Biol. Sex Differ. 4, 10.
Santoni, M., Sagheddu, C., Serra, V., Mostallino, R., Castelli, M.P., Pisano, F., Scherma, M., Fadda, P., Muntoni, A.L., Zamberletti, E., Rubino, T., Melis, M., Pistis, M., 2023. Maternal immune activation impairs endocannabinoid signaling in the mesolimbic system of adolescent male offspring. Brain Behav. Immun. 109, 271–284.
Scattoni, M.L., Martire, A., Cartocci, G., Ferrante, A., Ricceri, L., 2013. Reduced social interaction, behavioural flexibility and BDNF signalling in the BTBR T+ tf/J strain, a mouse model of autism. Behav. Brain Res. 251, 35–40.
Schaer, R., Wenger, N., Herrero, F., Notter, T., Meyer, U., 2025. Ontogeny and plasticity of resilience and susceptibility in a mouse model of maternal immune activation. Brain Behav. Immun. 129, 666–680.
Schafer, D.P., Lehrman, E.K., Kautzman, A.G., Koyama, R., Mardinly, A.R., Yamasaki, R., Ransohoff, R.M., Greenberg, M.E., Barres, B.A., Stevens, B., 2012. Microglia sculpt postnatal neural circuits in an activity and complement-dependent manner. Neuron 74, 691–705.
Semple, B.D., Blomgren, K., Gimlin, K., Ferriero, D.M., Noble-Haeusslein, L.J., 2013. Brain development in rodents and humans: Identifying benchmarks of maturation and vulnerability to injury across species. Prog. Neurobiol. 106–107, 1–16.
Servadio, M., Melancia, F., Manduca, A., di Masi, A., Schiavi, S., Cartocci, V., Pallottini, V., Campolongo, P., Ascenzi, P., Trezza, V., 2016. Targeting anandamide metabolism rescues core and associated autistic-like symptoms in rats prenatally exposed to valproic acid. Transl. Psychiatry 6, e902.
Sonninen, T.M., Goldsteins, G., Laham-Karam, N., Koistinaho, J., Lehtonen, S., 2020. Proteostasis Disturbances and Inflammation in Neurodegenerative Diseases. Cells 9.
Sorrells, S.F., Caso, J.R., Munhoz, C.D., Sapolsky, R.M., 2009. The stressed CNS: when glucocorticoids aggravate inflammation. Neuron 64, 33–39.
Spagnuolo, M.S., Donizetti, A., Iannotta, L., Aliperti, V., Cupidi, C., Bruni, A.C., Cigliano, L., 2018. Brain-derived neurotrophic factor modulates cholesterol homeostasis and Apolipoprotein E synthesis in human cell models of astrocytes and neurons. J. Cell. Physiol. 233, 6925–6943.
Spagnuolo, M.S., Maresca, B., Mollica, M.P., Cavaliere, G., Cefaliello, C., Trinchese, G., Esposito, M.G., Scudiero, R., Crispino, M., Abrescia, P., Cigliano, L., 2014. Haptoglobin increases with age in rat hippocampus and modulates Apolipoprotein E mediated cholesterol trafficking in neuroblastoma cell lines. Front. Cell. Neurosci. 8, 212.
Sungur, A.O., Vorckel, K.J., Schwarting, R.K., Wohr, M., 2014. Repetitive behaviors in the Shank1 knockout mouse model for autism spectrum disorder: developmental aspects and effects of social context. J. Neurosci. Methods 234, 92–100.
Talukdar, P.M., Abdul, F., Maes, M., Berk, M., Venkatasubramanian, G., Kutty, B.M., Debnath, M., 2021. A proof-of-concept study of maternal immune activation mediated induction of Toll-like receptor (TLR) and inflammasome pathways leading to neuroprogressive changes and schizophrenia-like behaviours in offspring. Eur. Neuropsychopharmacol. 52, 48–61.
Tartaglione, A.M., Cipriani, C., Chiarotti, F., Perrone, B., Balestrieri, E., Matteucci, C., Sinibaldi-Vallebona, P., Calamandrei, G., Ricceri, L., 2019. Early behavioral alterations and increased expression of endogenous retroviruses are inherited across generations in mice prenatally exposed to valproic acid. Mol. Neurobiol. 56, 3736–3750.
Tartaglione, A.M., Villani, A., Ajmone-Cat, M.A., Minghetti, L., Ricceri, L., Pazienza, V., De Simone, R., Calamandrei, G., 2022. Maternal immune activation induces autism-like changes in behavior, neuroinflammatory profile and gut microbiota in mouse offspring of both sexes. Transl. Psychiatry 12, 384.
Taurines, R., Segura, M., Schecklmann, M., Albantakis, L., Grunblatt, E., Walitza, S., Jans, T., Lyttwin, B., Haberhausen, M., Theisen, F.M., Martin, B., Briegel, W., Thome, J., Schwenck, C., Romanos, M., Gerlach, M., 2014. Altered peripheral BDNF mRNA expression and BDNF protein concentrations in blood of children and adolescents with autism spectrum disorder. J. Neural Transm. (Vienna) 121, 1117–1128.
Thomas, A., Burant, A., Bui, N., Graham, D., Yuva-Paylor, L.A., Paylor, R., 2009. Marble burying reflects a repetitive and perseverative behavior more than novelty-induced anxiety. Psychopharmacology 204, 361–373.
Toscano, C.V.A., Barros, L., Lima, A.B., Nunes, T., Carvalho, H.M., Gaspar, J.M., 2021. Neuroinflammation in autism spectrum disorders: Exercise as a “pharmacological” tool. Neurosci. Biobehav. Rev. 129, 63–74.
Tremblay, M.E., Stevens, B., Sierra, A., Wake, H., Bessis, A., Nimmerjahn, A., 2011. The role of microglia in the healthy brain. J. Neurosci. 31, 16064–16069.
Wang, H., 2014. Lipid rafts: a signaling platform linking cholesterol metabolism to synaptic deficits in autism spectrum disorders. Front. Behav. Neurosci. 8, 104.
Wang, X., Li, Q., Lyu, Z., Wu, Y., 2025. Supplementing with vitamin D during pregnancy reduces inflammation and prevents autism-related behaviors in offspring caused by maternal immune activation. Biol. Pharm. Bull. 48, 632–640.
Weinhard, L., di Bartolomei, G., Bolasco, G., Machado, P., Schieber, N.L., Neniskyte, U., Exiga, M., Vadisiute, A., Raggioli, A., Schertel, A., Schwab, Y., Gross, C.T., 2018. Microglia remodel synapses by presynaptic trogocytosis and spine head filopodia induction. Nat. Commun. 9, 1228.
Wilson, R.B., Enticott, P.G., Rinehart, N.J., 2018. Motor development and delay: advances in assessment of motor skills in autism spectrum disorders. Curr. Opin. Neurol. 31, 134–139.
Winden, K.D., Ruiz, J.F., Sahin, M., 2025. Construction destruction: Contribution of dyregulated proteostasis to neurodevelopmental disorders. Curr. Opin. Neurobiol. 90, 102934.
Wolf, Y., Yona, S., Kim, K.W., Jung, S., 2013. Microglia, seen from the CX3CR1 angle. Front. Cell. Neurosci. 7, 26.
Won, S., Levy, J.M., Nicoll, R.A., Roche, K.W., 2017. MAGUKs: multifaceted synaptic organizers. Curr. Opin. Neurobiol. 43, 94–101.
Wong, H., Hoeffer, C., 2018. Maternal IL-17A in autism. Exp. Neurol. 299, 228–240.
Wu, H., Wang, X., Gao, J., Liang, S., Hao, Y., Sun, C., Xia, W., Cao, Y., Wu, L., 2017. Fingolimod (FTY720) attenuates social deficits, learning and memory impairments, neuronal loss and neuroinflammation in the rat model of autism. Life Sci. 173, 43–54.
Xuan, I.C., Hampson, D.R., 2014. Gender-dependent effects of maternal immune activation on the behavior of mouse offspring. PLoS One 9, e104433.
Yang, L.G., March, Z.M., Stephenson, R.A., Narayan, P.S., 2023. Apolipoprotein E in lipid metabolism and neurodegenerative disease. Trends Endocrinol Metab 34, 430–445.
Yotova, A.Y., Li, L.L., O'Leary, A., Tegeder, I., Reif, A., Courtney, M.J., Slattery, D.A., Freudenberg, F., 2024. Synaptic proteome perturbations after maternal immune activation: Identification of embryonic and adult hippocampal changes. Brain Behav. Immun. 121, 351–364.

Yuan, J., Wang, L., Lin, Y., Chen, J., Hu, J., 2015. Differences of plasma IL-1 and TNF-alpha in healthy Chinese Population. Open Med (wars) 10, 306–310.
Zanda, M.T., Fadda, P., Antinori, S., Di Chio, M., Fratta, W., Chiamulera, C., Fattore, L., 2017. Methoxetamine affects brain processing involved in emotional response in rats. Br. J. Pharmacol. 174, 3333–3345.
Zheng, Z., Zhang, L., Zhu, T., Huang, J., Qu, Y., Mu, D., 2016. Peripheral brain-derived neurotrophic factor in autism spectrum disorder: a systematic review and meta-analysis. Sci. Rep. 6, 31241.